

1
2
3
4
5
6
7

Millennial-scale climate oscillations triggered by deglacial meltwater discharge in last glacial maximum simulations

Yvan M. Romé¹, Ruza F. Ivanovic¹, Lauren J. Gregoire¹, Sam
Sherriff-Tadano¹, Paul J. Valdes²

¹School of Earth and Environment, University of Leeds, Leeds, UK
²School of Geographical Sciences, University of Bristol, Bristol, UK

Corresponding author: Yvan Romé, eeymr@leeds.ac.uk

8 Abstract

9 Our limited understanding of millennial-scale variability in the context of the last glacial
 10 period can be explained by the lack of a reliable modelling framework to study abrupt
 11 climate changes under realistic glacial backgrounds. In this article, we describe a new
 12 set of long-run Last Glacial Maximum experiments where such climate shifts were trig-
 13 gered by different snapshots of ice-sheet meltwater derived from the early stages of the
 14 last deglaciation. Depending on the location and the magnitude of the forcing, we ob-
 15 serve three distinct dynamical regimes and highlight a subtle window of opportunity where
 16 the climate can sustain oscillations between cold and warm modes. We identify the European-
 17 Arctic and Nordic Seas regions as being most sensitive to meltwater discharge in the con-
 18 text of switching to a cold mode, compared to freshwater fluxes from the Laurentide ice
 19 sheets. These cold climates follow a consistent pattern in temperature, sea ice and con-
 20 vection, and are largely independent from freshwater release as a result of effective AMOC
 21 collapse. Warm modes, on the other hand, show more complexity in their response to
 22 the regional pattern of the meltwater input, and within them, we observe significant dif-
 23 ferences linked to the reorganisation of deep water formation sites and the subpolar gyre.
 24 Broadly, the main characteristics of the oscillations, obtained under full-glacial condi-
 25 tions with realistically low meltwater discharge, are comparable to $\delta^{18}O$ records of the
 26 last glacial period, although our simplified experiment design prevents detailed conclu-
 27 sions from being drawn on whether these represent actual Dansgaard-Oeschger events.

28 Plain Language Summary

29 During the last glacial period (115,000 to 12,000 years before present), the base-
 30 line cold climate was continuously disturbed by intense and abrupt climate changes. They
 31 completely modified the climate for a few thousand years or so, resulting, for instance,
 32 in massive temperature shifts and complete reorganisations of ocean circulation. These
 33 abrupt changes have been observed in climate records from the Northern Hemisphere
 34 and also can be traced in records from the Southern Hemisphere. Yet, we still do not
 35 know what triggers these changes, and often cannot simulate them at the right time un-
 36 der known environmental conditions. In the context of the Last Glacial maximum, a cold
 37 period 21,000 years ago with extensive ice over the Northern Hemisphere, this article anal-
 38 yses a new set of climate model simulations that test the effects of freshwater melting
 39 from the ice sheets at different periods of the early deglaciation (\sim 21,000 to 18,000 years
 40 before present). Under some conditions, the resulting experiments displayed an Atlantic
 41 Ocean that oscillates between strong and collapsed basin-wide circulation, causing ap-
 42 proximately 10°C of temperature change over Greenland; a behaviour that resembles ob-
 43 served abrupt climate changes.

44 1 Introduction

45 The last glacial period was characterised by strong millennial-scale variability (e.g.
 46 Bigg & Wadley, 2001; Wolff et al., 2010; Fletcher et al., 2010), observed through the oc-
 47 currence of sharp and dramatic shifts in climate state. The best example of such abrupt
 48 changes are Dansgaard-Oeschger events (D-O events; Dansgaard et al., 1993). They con-
 49 sist of transitions between cold stadial and warm interstadial climate conditions that oc-
 50 cur in cycles as long as six hundred to a few thousand years. Dansgaard-Oeschger events
 51 were first identified in $\delta^{18}O$ records of Greenland ice cores (Bond et al., 1993) before also
 52 being observed in Antarctica (Blunier & Brook, 2001; Voelker, 2002). Since their dis-
 53 covery, they have been identified in a wide range of different parts of the Earth system,
 54 both marine (e.g. Shackleton et al., 2000; Wolff et al., 2010; Dokken et al., 2013; Henry
 55 et al., 2016) and terrestrial (e.g. Goñi et al., 2000; Y. J. Wang et al., 2001; X. Wang et
 56 al., 2007; Margari et al., 2009; Stockhecke et al., 2016), and can be linked to meridional
 57 shifts of the Intertropical Convergence Zone (ITCZ; Peterson & Haug, 2006).

58 During decades of study, numerous hypotheses have been put forward to under-
59 stand the underlying mechanisms behind D-O events (a comprehensive list can be found
60 in Li and Born (2019)), and, more generally, millennial scale variability, yet they remain
61 largely unexplained. Nonetheless, at the crossroads of all theories lies the crucial role of
62 the Atlantic Meridional Overturning Circulation (AMOC) (Rahmstorf, 2002; Burckel et
63 al., 2015; Henry et al., 2016). A modification of the thermohaline circulation affects heat
64 and salt redistribution between the tropics and the poles, and consequently has a global-
65 scale impact on the climate (Clark et al., 2002; Rahmstorf, 2002). There is substantial
66 evidence that the AMOC has existed in other configurations (or ‘modes’) than the one
67 we observe at present times (e.g. Böhm et al., 2015), and that AMOC may thus have
68 the capacity to exist in multiple stable states, as predicted theoretically (Stommel, 1961)
69 and supported by early observations (Broecker et al., 1985) and climate models (Manabe
70 & Stouffer, 1988). Our understanding of abrupt climate change, therefore, relies on un-
71 covering the cause of AMOC mode switches.

72 The AMOC can be disrupted by freshwater release events in the North Atlantic-
73 Arctic region. They have the power to target vital points of the thermohaline circula-
74 tion by affecting the ocean density profile at North Atlantic Deep Water (NADW) for-
75 mation sites (Broecker et al., 1985; Paillard & Labeyriet, 1994; Vidal et al., 1997). In
76 models, freshwater hosing experiments have been widely used to force abrupt climate tran-
77 sitions (e.g. Manabe & Stouffer, 1997; Ganopolski & Rahmstorf, 2001; Kageyama et al.,
78 2010) and observe hysteresis cycles (e.g. Schmittner et al., 2002). They also highlighted
79 the large sensitivity of the climate to the strength and the location of the release, espe-
80 cially in the Greenland, Iceland and Nordic (GIN) Seas (Smith & Gregory, 2009; Roche
81 et al., 2010). Consequently, it is valuable to explore the different sources of freshwater
82 that had the potential to lead to millennial-scale variability.

83 Iceberg surges during Heinrich events (H events; Heinrich, 1988) recorded by Ice
84 Rafted Debris (IRD) in the North Atlantic (Hemming, 2004), were first candidate to be
85 held responsible for initiating stadial climates. It is now widely accepted that H events
86 are not at the origin of D-O events, they are triggered within stadial states (Barker et
87 al., 2015) and are not recorded at every D-O occurrence (Lynch-Stieglitz, 2017). Instead,
88 we can conceive of them as a likely response to the earlier climate-ocean perturbation
89 or even a positive feedback mechanism for perpetuating/amplifying stadial climates (Ivanovic
90 et al., 2018). Meltwater released from the long term deglaciation of ice sheets was an-
91 other significant source of freshwater during the last glacial period (Gregoire et al., 2012),
92 although only a few studies have investigated the influence of such ‘background’ melt
93 (e.g. Ivanovic et al., 2018; Kapsch et al., 2022; Matero et al., 2017), probably because
94 it requires precise constraints on the ice sheet geometry and history of melt/growth (Bethke
95 et al., 2012). Holding the most complete records of ice sheet evolution, both in terms of
96 spatial and temporal resolution, (e.g. Dyke, 2004; Hughes et al., 2016; Briggs et al., 2014;
97 Bradwell et al., 2021), the last deglaciation (and especially its early phase, ~ 21 –16 ka
98 BP, thousand years before present) offers the perfect setting to assess the ability of the
99 early phase of continental deglaciation (i.e. the long-term background melt from disin-
100 tegrating ice sheets) to generate millennial-scale variability in glacial conditions.

101 The last deglaciation initiated from the Last Glacial Maximum (LGM; ~ 21 ka,
102 (Clark et al., 2009), which corresponds to a maximum in continental ice sheet extent in
103 the Northern Hemisphere (Batchelor et al., 2019) shaped during the preceding glacial
104 period. The upper cell of the AMOC was likely shallower, but it is not known whether
105 it was stronger or weaker than present day (Gebbie, 2014; Lynch-Stieglitz, 2017; Muglia
106 & Schmittner, 2021). A steady increase in Northern Hemisphere summer insolation (Berger,
107 1978) triggered the long-term demise of the Laurentide and Eurasian ice sheets, with ris-
108 ing concentrations of atmospheric CO₂ positively reinforcing the deglaciation (Gregoire
109 et al., 2015). However, while Southern Hemisphere temperatures gradually rose (Parrenin
110 et al., 2007), the climate in the North remained cold for several thousand years; a pe-

111 rioid known as Heinrich Stadial 1 (~ 18 – 15 ka BP) (Denton et al., 2006; Roche et al., 2011;
112 Ng et al., 2018). The most recent of Heinrich events, H1 (Hemming, 2004; Stanford et
113 al., 2011), began some two thousand years after the onset of Heinrich Stadial 1 (Stern
114 & Lisiecki, 2013; Hodell et al., 2017). In the years of deglaciation that followed the LGM,
115 several millennial scale events were observed (Weber et al., 2014). Two episodes are par-
116 ticularly relevant to our study: the sudden Bølling Warming (~ 14.5 – 13 ka BP; Sever-
117 inghaus & Brook, 1999) concurrent with an intensification of the AMOC (Ng et al., 2018;
118 Du et al., 2020), and the ensuing Younger Dryas, when Northern Hemisphere climate
119 abruptly returned to a stadial state with glacial re-advance (~ 13 – 12 ka; Murton et al.,
120 2010; Liu et al., 2012). While not formally identified as D-O events, similarities in cli-
121 mate and ocean evolution between these last deglaciation and D-O oscillations have prompted
122 others to at least draw analogies between them, and to speculate on whether they have
123 a common cause (e.g. Obase & Abe-Ouchi, 2019).

124 Simulating climate oscillations in glacial conditions has proven to be very challeng-
125 ing, and even more so during the LGM. This is because of the strong feedback between
126 the large ice sheets and wind stress, deep water formation and energy balance (Oka et
127 al., 2012; Ullman et al., 2014; Beghin et al., 2015; Roberts & Valdes, 2017), which act
128 to intensify, or at least stabilise, the AMOC (Oka et al., 2012; Klockmann et al., 2016;
129 Sherriff-Tadano et al., 2018). Most models from both the Paleoclimate Modelling Inter-
130 comparison Project Phase 3 (PMIP3; Muglia & Schmittner, 2015) and Phase 4 (PMIP4;
131 Kageyama et al., 2021) tend to simulate a deeper and stronger NADW than inferred from
132 palaeo records, which could explain why few modelling studies have observed millennial
133 scale variability in glacial background (e.g. Klockmann et al., 2018). In order to trig-
134 ger abrupt climate transitions, freshwater hosing experiments have historically needed
135 to overestimate fluxes as reviewed by Kageyama et al. (2010) (e.g. Liu et al., 2009; Men-
136 viel et al., 2011), and have not succeeded in simulating abrupt changes when using ‘re-
137 alistic’ fluxes (Bethke et al., 2012; Gregoire et al., 2012; Snoll et al., 2022). Obase and
138 Abe-Ouchi (2019) have arguably come the closest to overcoming this meltwater ‘para-
139 dox’ by simulating the Bølling Warming even with some deglacial meltwater forcing. How-
140 ever, even they require a significantly lower than likely freshwater discharge from the deglaci-
141 ating ice sheets (e.g. Peltier et al., 2015).

142 The dispute over what could feasibly cause abrupt climate changes not directly driven
143 by freshwater fluxes led the community to start actively searching for oscillating behaviours
144 in their models. At the same time, the criticism that simulations integrated for only a
145 few hundred or a thousand years should not be considered to have a steady-state or ‘spun-
146 up’ ocean circulation began to gain traction (Marzocchi & Jansen, 2017; Dentith et al.,
147 2019), prompting modellers to run long simulations with higher-order climate models —
148 made possible by the increase of computational power — in order to examine long-term
149 drifts. It is therefore probably not a coincidence that more and more coupled Atmosphere-
150 Ocean General Circulation Models (AOGCMs) have reported observing AMOC mode
151 oscillations in recent years (e.g. Peltier & Vettoretti, 2014; Brown & Galbraith, 2016;
152 Klockmann et al., 2018; Sherriff-Tadano & Abe-Ouchi, 2020). They have been achieved
153 under a range of different freshwater hosing scenarios (e.g. Cheng et al., 2011), atmo-
154 spheric CO_2 concentrations (e.g. Zhang et al., 2017) and ice sheet geometries (e.g. Klock-
155 mann et al., 2018), although, to our knowledge, only Peltier and Vettoretti (2014) man-
156 aged to obtain AMOC oscillations under glacial maximum conditions.

157 To sum-up the combined results from these studies, there seems to exist a window
158 of opportunity (Barker & Knorr, 2021) in each model’s inputs (parameter values, bound-
159 ary conditions and forcings) and background climates where oscillations can establish
160 and sustain (e.g. Peltier & Vettoretti, 2014; Brown & Galbraith, 2016; Klockmann et
161 al., 2018). The ice sheets’ layout in particular has a strong influence on the local and global
162 climate, including on the atmospheric circulation (Löffverström et al., 2014; Roberts et
163 al., 2014; Sherriff-Tadano et al., 2021), the gyres (Gregoire et al., 2018), the energy bal-

164 ance (Roberts & Valdes, 2017) and freshwater fluxes (Matero et al., 2017). As a result,
165 the new generation of better constrained and more detailed ice sheet reconstructions such
166 as ICE-6G_C (Peltier et al., 2015; Argus et al., 2014) and GLAC-1D (Tarasov & Peltier,
167 2002; Tarasov et al., 2012; Briggs et al., 2014; Ivanovic et al., 2016) may prove to be de-
168 cisive in whether or not the ‘right’ conditions for triggering abrupt climate changes are
169 obtained.

170 In this paper, we present our contribution to this initiative in the form of a new
171 set of LGM simulations forced with deglacial meltwater. Inspired by an initial experi-
172 ment that showed millennial-scale variability under a transient meltwater forcing, we de-
173 signed our simulations with fixed meltwater inputs in order to be able to describe the
174 oscillations in detail and evaluate the sensitivity of the oscillatory behaviour to meltwa-
175 ter patterns. These inputs were derived from snapshots of the early deglaciation melt-
176 water history (specifically, between 21.5 and 17 ka BP) calculated from GLAC-1D ice
177 sheet reconstruction.

178 Depending on the freshwater pattern, we observe three different dynamical regimes,
179 including regular and self-sustained climate oscillations. The oscillations are characterised
180 by switches between strong, shallow glacial AMOC and near- or completely- collapsed
181 AMOC modes, a Greenland surface cooling/warming of $\sim 10^\circ\text{C}$, and a periodicity of about
182 1,500 ka. This regime can be sustained for about 10,000 years (the maximum length of
183 the experiments). These are, to our knowledge, the first general circulation model sim-
184 ulations to use ice sheet reconstruction-derived distributions of meltwater to produce strong
185 AMOC oscillations under glacial maximum climate conditions, and to investigate the sen-
186 sitivity of the oscillations to patterns of meltwater discharged to the ocean.

187 The non-oscillating clusters of our experiments inform us of the pre-requisite con-
188 ditions for passing through the oscillating window. Here, we describe the various sim-
189 ulations in detail, their oscillatory or non-oscillatory climate/ocean states, and the dif-
190 ferent Earth system components involved in the abrupt events. We conclude with a dis-
191 cussion on the relevance of our simulations in the context of known past abrupt climate
192 changes. The design introduced in this study allows us to undertake a relatively system-
193 atic set of sensitivity tests of the impact of realistic freshwater distributions (albeit for
194 unrealistic lengths of time) on ocean circulation, with the multi-millennial integrations
195 enabling us to explore the long-term effect of each pattern.

196 2 Methods

197 2.1 The model

198 The simulations introduced in this article were completed using the BRIDGE (Bris-
199 tol Research Initiative for the Dynamic Global Environment group) version of the HadCM3
200 atmosphere-ocean general circulation model (GCM) (Valdes et al., 2017). This GCM con-
201 sists of a 19 layers $\times 2.5^\circ \times 3.75^\circ$ atmosphere model more completely described by Pope
202 et al. (2000), coupled every simulation day with a 20 layers (up to 5,500m deep) $\times 1.25^\circ$
203 $\times 1.25^\circ$ ocean model, described by Gordon et al. (2000) (Bryan & Cox, 1972; Fofonoff
204 & Millard Jr, 1983; Fofonoff, 1985). This version of HadCM3 includes the MOSES 2.1
205 land model (P. M. Cox et al., 1999), and the TRIFFID dynamic vegetation model (P. Cox,
206 2001). HadCM3 has been tested in many different scenarios (I.P.C.C., 2014; Reichler &
207 Kim, 2008), and was optimised for running multi-millennial simulations (Valdes et al.,
208 2017).

209 2.2 Experimental design

210 The LGM simulation that makes up the base climate state for all simulations pre-
211 sented here was created following the PMIP4 protocol for 21 ka BP (Kageyama et al.,

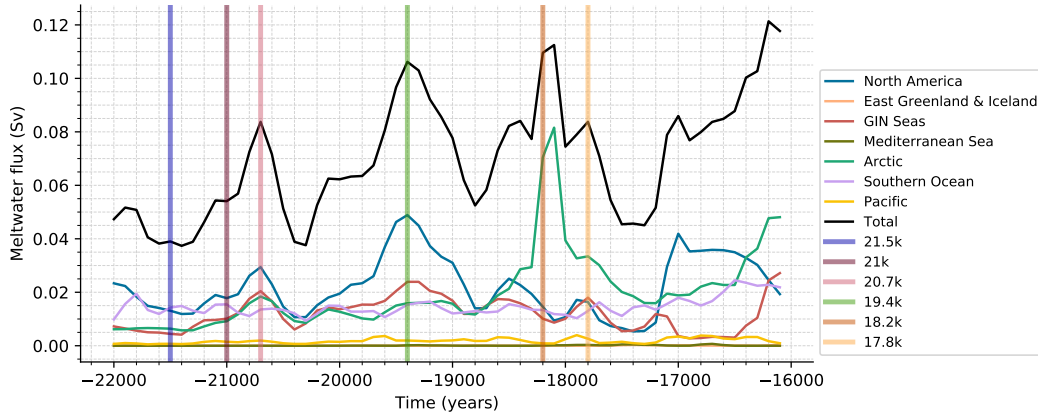


Figure 1. Meltwater discharge history over the early deglaciation and its distribution over key regions (defined in Figure S2b). This plot incorporates the 200-years smoothing described in section S2. Vertical bars represent the time steps chosen for calculating each constant meltwater-forcing snapshot (see section 2.2, and Table 1).

212 2017) using the GLAC-1D ice sheet reconstruction (Tarasov & Peltier, 2002; Tarasov et
 213 al., 2012; Briggs et al., 2014; Ivanovic et al., 2016); see section S1 (Bereiter et al., 2015;
 214 Loulergue et al., 2008; Schilt et al., 2010). This new HadCM3 LGM simulation was ini-
 215 tialised from a chain of existing multi-millennial HadCM3 PMIP3 LGM simulations, which
 216 were started from multi-millennial continuations of earlier HadCM3 LGM simulations
 217 (Davies-Barnard et al., 2017), giving a pre-PMIP4 LGM spin-up of several thousand years.
 218 The new PMIP4 GLAC-1D set-up was integrated for 3,500 years, and the end of this fi-
 219 nal spin-up phase provides the initial condition for all simulations presented here. We
 220 continued the LGM simulation for a further 4,000 years in parallel with our other ex-
 221 periments to provide a reference climate state (*CTRL*) for comparison to the other sim-
 222 ulations. There are small, steady drifts in the ocean over the run (Figure S5), but the
 223 signal of the trends are dwarfed in comparison to the changes of interest described be-
 224 low, and little is gained for this study by extending *CTRL* further. The starting year of
 225 *CTRL* is defined as year 0.

226 GLAC-1D has rarely been used for LGM simulations compared to the other ice sheet
 227 reconstructions (Kageyama et al., 2021) such as ICE-6G_C (Peltier et al., 2015) and the
 228 PMIP3 ice sheet (Abe-Ouchi et al., 2015). It was preferred for this study because com-
 229 pared to the alternative reconstructions, it includes more recent constraints on the Eurasian
 230 ice sheets (provided by the DATED-1 project; (Hughes et al., 2016), a region that could
 231 be crucial for accurately capturing the early deglacial climate history (Ivanovic et al.,
 232 2018). A transient meltwater history was derived from GLAC-1D’s representation of the
 233 deglaciation (section S2). We decided against using the transient meltwater flux, because
 234 the added complexity introduced by the temporal variability and possible ocean ‘mem-
 235 ory’ of the preceding [uncertain] meltwater history would have convoluted the physical
 236 interpretation of our results. Instead, we examined the triggering of abrupt climate changes
 237 using a simpler approach; by selecting six interesting, different, fixed-forcing scenarios
 238 (our ‘snapshots’), that allow us to investigate the sensitivity of the glacial ocean and sur-
 239 face climate to early deglacial freshwater inputs (Figure 1).

240 The snapshots were identified for their ability to collectively capture a broad range
 241 of possible situations that may have led to changes in ocean circulation and surface cli-
 242 mate. The six scenarios correspond to different modes of discharge and are named af-
 243 ter the period they were extracted from (see Figure 1); see Figure S2c for the spatial dis-

Simulation	Meltwater (Total flux)	Integration length	Category	Salinity Target (PSU)
<i>CTRL</i>	None	4,000 years	reference	35.8334
<i>21.5k</i>	21.5 ka (0.039 Sv)	4,000 years	warm	35.834
<i>21k</i>	21 ka (0.054 Sv)	4,000 years	warm	35.8334
<i>20.7k</i>	20.7 ka (0.084 Sv)	10,000 years	oscillating	35.8225
<i>19.4k</i>	19.4 ka (0.106 Sv)	10,000 years	oscillating	35.7901
<i>18.2k</i>	18.2 ka (0.109 Sv)	10,000 years	slow-recovery	35.7348
<i>17.8k</i>	17.8 ka (0.084 Sv)	10,000 years	oscillating	35.7125

Table 1. Experiments summary. All experiments were designed with LGM boundary conditions, using the LGM GLAC-1D ice sheet extent and associated geographies. Entries in the *Category* and global mean *Salinity Target (PSU)* columns are explained in sections 4 and 2.2, respectively.

244 tribution of the fluxes. The *21.5k*, *21k* and *20.7k* snapshots were chosen for being close
245 to the LGM, sharing a similar distribution, but with different rates of meltwater discharge.
246 The *19.4k* snapshot hosts a strong Labrador Sea/North Eastern American coast/Gulf
247 of Mexico discharge (shortened to ‘North American’ discharge hereafter), but has a rela-
248 tively small meltwater flux to the Arctic. Conversely, *18.2k* and *17.8k* have high Arc-
249 tic and low North Atlantic discharge, with *18.2k* having the most freshwater entering
250 the Arctic. These six snapshots of the deglacial meltwater history were used as forcing
251 for six new equilibrium-type (i.e. constant-forcing) simulations, started from year 0. The
252 meltwater inputs were kept constant throughout the runs.

253 Table 1 presents a summary of all experiments. The difference between any of them
254 is the prescribed ice sheet meltwater (or absence of it, in *CTRL*).

255 The idea of having a continuous fixed meltwater discharge for thousands of years
256 is unrealistic by nature. However, in the most extreme scenario (*18.2k*), the total forc-
257 ing corresponds to a sea level rise of 102 m in 10,000 years, which, for context, is still
258 less than what has been reconstructed for the whole of the last deglaciation (Lambeck
259 et al., 2014). It therefore remains appropriate to consider our results in light of glacial
260 and deglacial variability in order to understand the effect of the forcing, though we are
261 careful to highlight that this is not a transient simulation of deglacial meltwater. To avoid
262 long-term drifts in mean ocean salinity caused by the long freshwater forcing, we impose
263 a constant global mean salinity target (following the *VFLUX* method of Dentith et al.
264 (2019) commensurate with the starting condition for each ‘snapshot’ (Table 1). The salin-
265 ity target conserves water in relation to terrestrial ice volume (applied as relative to the
266 present day) and thus, in the context of these simulations, counteracts global freshen-
267 ing by removing the excess water as a very small proportion of freshwater from every ocean
268 grid cell at every ocean model timestep (one hour). This approach is in keeping with the
269 snapshot/equilibrium experimental design whilst still allowing the ocean to ‘feel’ the sur-
270 face forcing. See section S3 for details.

271 Most simulations were run for 10,000 years; long enough to characterise their cli-
272 mate behaviours. However, like *CTRL*, two simulations (*21.5k* and *20.7k*), were termi-
273 nated after 4,000 years. At this point, little was changing in those simulations, and since
274 no further time series were required for the analysis, we opted to conserve the comput-
275 ing resource.

276 Some simulations experienced numerical instability in the stream function off the
277 coast of the Philippines after a few thousand years. This quirk was resolved by smooth-
278 ing the bathymetry in the region of the instability and restarting the run a few years be-

fore the instability arose. More information, including the detail of the smoothing algorithm and its very minor impact on the climate response, is given in section S4.

2.3 Characterising oscillations and defining warm/cold-mode composites

All experiments apart from *CTRL* show some kind of alternation between weaker and stronger AMOC phases, or ‘modes’. Changes in the AMOC are correlated to increases and decreases in NGRIP temperatures (North Greenland Ice Core Project, 42.32° W, 75.01° N) and so we will also refer to these phases as ‘cold’ and ‘warm’ modes, respectively. We do not use the terms *stadial* and *interstadial* to describe the cold and warm states because of the complicated connotations associated with these terms, but they may be thought of in such a light.

In order to characterise oscillations in the simulations, we applied a filtering algorithm and Fourier analysis to derive the spectrum of the temperature time series at the location of NGRIP, see section S5 for details. If there is a peak in the spectrum, then oscillations can be defined and described, and we we apply a Butterworth low-pass filter to screen-out the frequencies lower than the millennial-scale variability of interest.

We also found it useful, in our analysis, to examine characteristics common to all warm and cold modes in the suite of simulations. Thus, to build a composite of the two modes from the time series of results, we defined quantitative boundaries bespoke to each simulation (it proved ineffective to adopt a consistent definition for all simulations because of their differences). Points below the weak limits (in AMOC strength/NGRIP temperature) were added to the composite cold mode and points above the strong limits were added to the warm modes. This approach is described in section S6, where we demonstrate that the choice of how to define the composite modes does not significantly impact the results, and that to manually set up the weak and strong limits was an easy and robust method to build the composite states.

3 A new weak, shallow AMOC LGM simulation

The *CTRL* run replicates and continues the HadCM3-GLAC-1D LGM simulation presented in Kageyama et al. (2021). The global mean surface temperature is 6.6°C colder than Pre-Industrial (PI). Compared to other PMIP4 simulations, this simulation is in the coolest range, almost 2°C below the average mean temperature, and is colder than any PMIP3 simulations analysed by Kageyama et al. (2021), yet close to the current estimate from global temperature reconstructions ($\sim 6.1^{\circ}\text{C}\pm 0.4^{\circ}\text{C}$ cooler than PI in Tierney et al. (2020), $\sim 7.0\pm 1.0^{\circ}\text{C}$ cooler than PI in Osman et al. (2021)). The global mean ocean surface temperature cools by 3.4°C, which is significantly cooler than the $\sim 1.7\pm 0.1^{\circ}\text{C}$ cooler than PI inferred by Paul et al. (2021), but again is a good match to the reconstruction by Tierney et al. (2020) ($\sim 3.1\pm 0.3^{\circ}\text{C}$ cooler than PI). Contrary to most PMIP4 models, HadCM3 produces an AMOC that is both shallower and weaker in a full-glacial background compared to its pre-industrial state, although AMOC is still vigorous with a maximum strength of 20 Sv at 30° N. We also note that the simulation gets slightly cooler when using GLAC-1D compared to ICE-6G_C (Ivanovic et al., 2018), despite similar values for the maximum overturning circulation.

A summary of the *CTRL* equilibrium climate is shown by Figure 2. The thermohaline circulation is fuelled by intense convection in the northeast Atlantic, with deep water formation sites located primarily south of Iceland and west of the British Isles (Figure 2b). This creates a corridor in the eastern part of the Atlantic where warm waters can transit to high latitudes, while the western part of the ocean gets covered by winter sea ice and observes a much cooler climate (Figure 2c). The winter sea ice layer extends towards the East of the North Atlantic basin, creating a strong North-South gra-

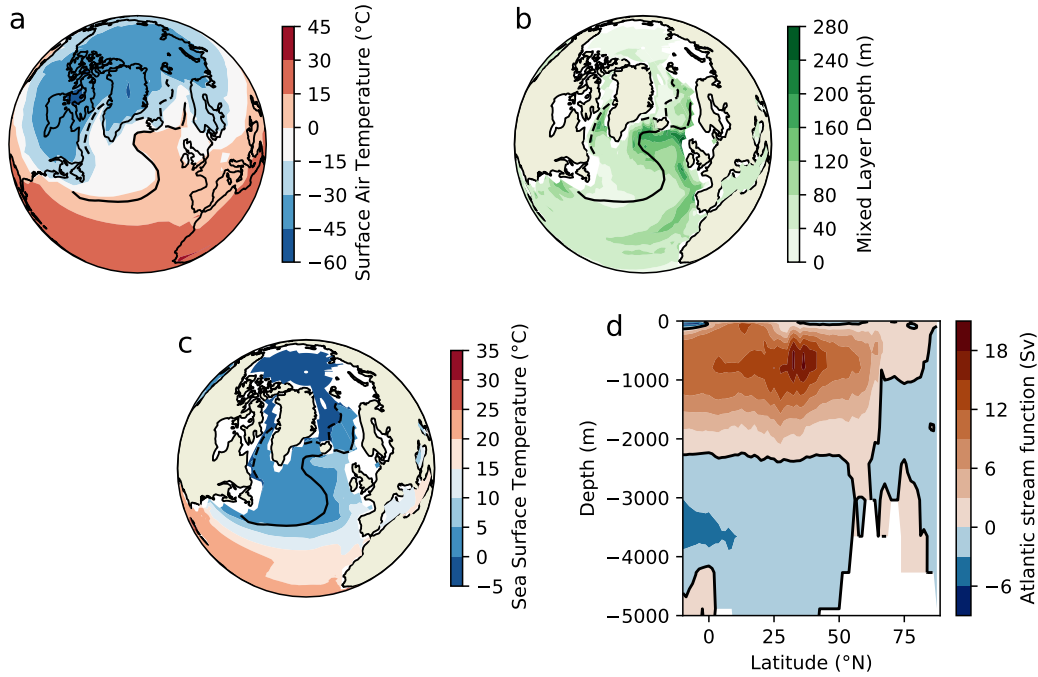


Figure 2. Mean annual conditions between simulation years 3900 and 4000 for *CTRL*. *a.* Surface air temperature. *b.* Mixed layer depth. *c.* Sea surface temperature. *d.* Meridional overturning stream function in the Atlantic basin. Dashed/solid lines indicate the March/September 50% sea-ice extent.

328 dient in atmospheric temperature in this region (Figure 2*a*). The Arctic Ocean is covered
 329 in sea ice all year long. Dense waters sink in the Labrador Sea when the sea ice is
 330 less extensive in this region in late autumn.

331 4 Climate response to the meltwater perturbations

332 We observe significant differences in the climate response of the six meltwater exper-
 333 iments (Figure 3), best encapsulated by the evolution of the AMOC index. For this
 334 study, we define the AMOC index as the maximal value of the overturning circulation
 335 in the Atlantic ocean at 26.5° N. This index corresponds to the modern RAPID-array
 336 AMOC measurement grid (Smeed et al., 2014) and has been regularly used in palaeo-
 337 studies (e.g. Guo et al., 2019).

338 The meltwater simulations can be assigned to three different regimes, or clusters,
 339 according to the AMOC index (Figure 3*b*). In the first grouping, simulations *21.5k* and
 340 *21k* returned to the reference state after a short cooling event during the initial years
 341 of the forcing, when the ocean adjusts to the introduction of the weak meltwater fluxes.
 342 This AMOC decline lasted for approximately 500 years, with the index weakening by
 343 as much as 5 Sv for *21k* and 1.5 Sv for *21.5k* approximately halfway through this ini-
 344 tial cooling. While *21.5k* hardly recorded a change of polar temperatures (Figure 3*c*),
 345 the drop in *21k* AMOC strength drives up to 5°C cooling over Greenland. Neither sim-
 346 ulation shows a strong response over Antarctica (Figure 3*d*). Accordingly, *21.5k* and *21k*
 347 will be referred to as *warm simulations* (note that with an LGM baseline climate, this
 348 term is relative).

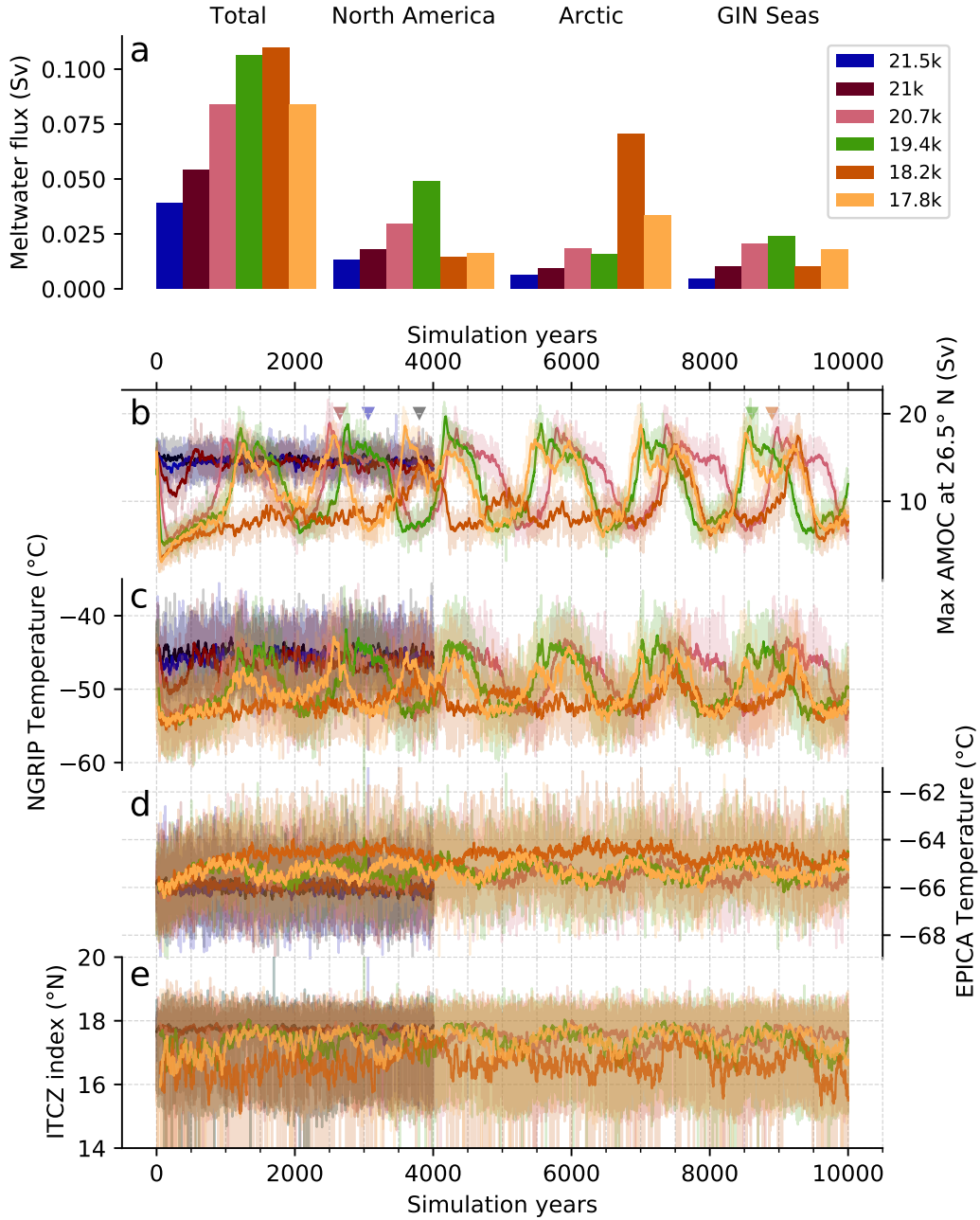


Figure 3. *a.* Snapshot experiments’ total meltwater discharge and distributions, summarised (the three main regions are defined in Figure S2). *b.* AMOC index (max Atlantic overturning circulation at 26.5° N). *c.* Greenland Surface Air Temperatures at NGRIP (42.32° W, 75.01° N). *d.* Antarctica Surface Air Temperatures at EPICA Dome C (Concordia Station of the European Project for Ice Coring in Antarctica, 123.21° E, 75.06° S). *e.* Intertropical Convergence Zone index (corresponding to the simulated mean Northern extent of the equatorial rain belt, defined in section S7, inspired by Braconnot et al. (2007) and Singarayer et al. (2017)). Solid lines represent the 30-years running mean and transparent envelopes represent inter-annual variability, except for panel *e*, where the solid line is the 50-year running mean for ease of readability. Arrows indicate the date of the application of localised bathymetric-smoothing (see section S4) for *21k*, *21.5k* and *CTRL* (left to right).

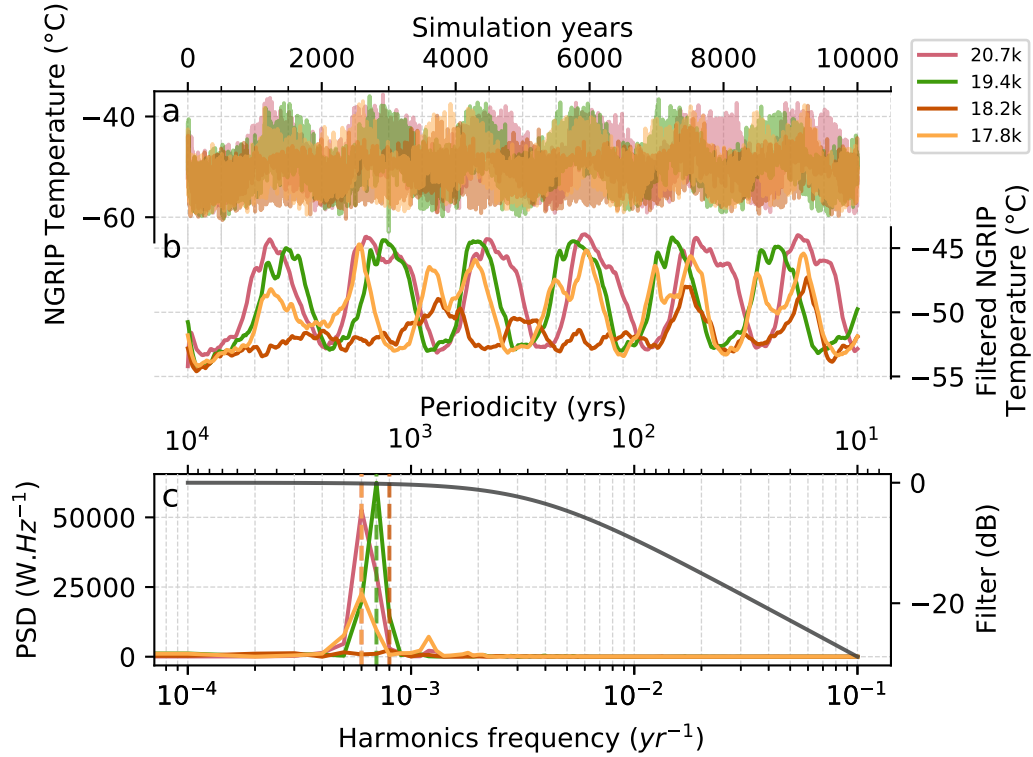


Figure 4. Spectral analysis of simulated surface air temperature through time above NGRIP (42.32° W, 75.01° N). *a.* Unfiltered signal for *oscillating* and *slow-recovery* simulations. *b.* Filtered response, using first class low-pass Butterworth filter. *c.* Power Spectral density (PSD, left hand scale) of the unfiltered signal. Dotted lines indicate the dominant frequency/period for each simulation. Grey line in panel *c* shows the bode diagram of the low-pass filter. Simulations *21.5k* and *21k* are not shown as their Fourier analysis was not conclusive.

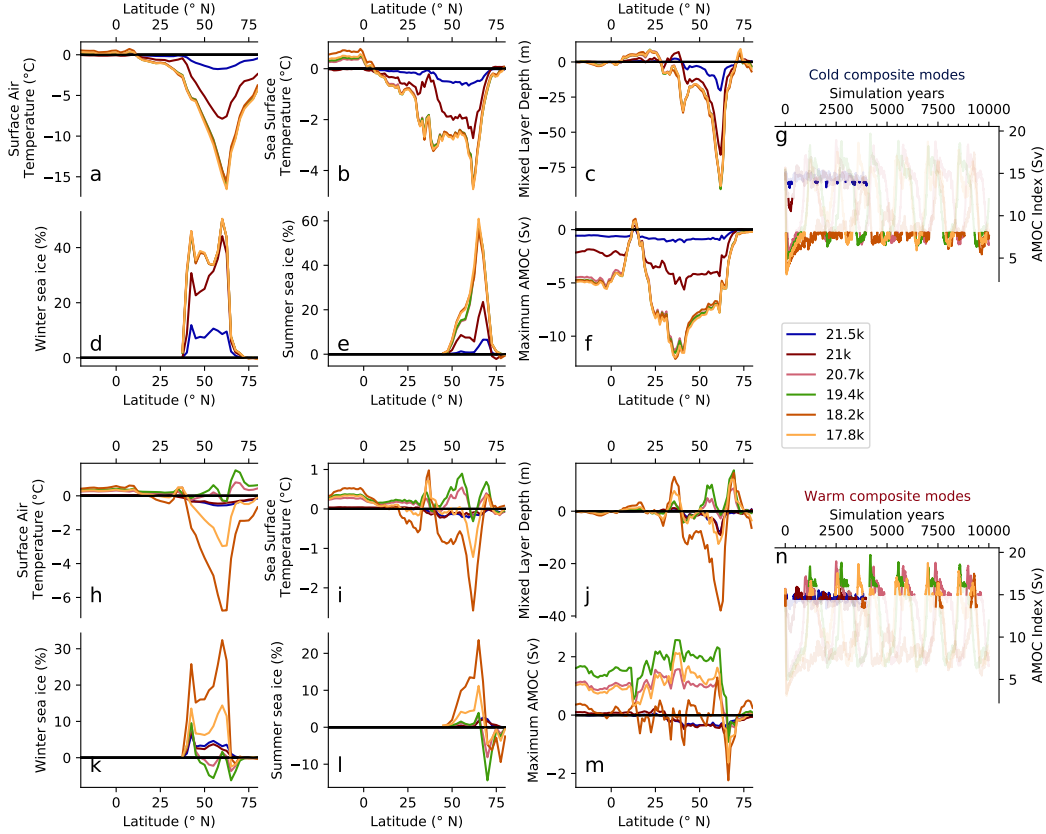


Figure 5. Composite cold and warm modes’ mean zonal anomalies between the meltwater simulations and the reference state in the Atlantic (70° W – 10° E). For cold modes (top), panels show the zonally averaged *a.* surface air temperature, *b.* sea surface temperature, *c.* mixed layer depth, *d.* winter sea ice concentration, *e.* summer sea ice and *f.* maximum overturning circulation flow over the water column. For warm modes (bottom), panels show the zonally averaged *h.* surface air temperature, *i.* sea surface temperature, *j.* mixed layer depth, *k.* winter sea ice concentration, *l.* summer sea ice and *m.* maximum overturning circulation flow over the water column. For orientation, an AMOC time series highlighting the periods contributing to the composite cold and warm modes is shown by panels *g* and *n*, respectively.

349 In a second regime of its own, the AMOC in *18.2k* almost entirely collapsed as soon
 350 as meltwater was discharged, causing Northern Hemisphere cooling and a significant shift
 351 southward of the ITCZ (Figure 3*e*). Short recovery episodes occur at irregular intervals
 352 through the 10,000 years of the simulation, but they cannot be sustained for longer than
 353 a few hundred years. This simulation will be labelled a *slow-recovery simulation*.

354 Finally, through Fourier analysis (Figure 4*c*; section 2.3) we identify three *oscil-*
 355 *lating simulations* (*20.7k*, *19.4k* and *17.8k*). They switch to a cold state at the onset of
 356 the run and continue in a quasi-oscillating regime between cold (near collapsed AMOC,
 357 similar to *18.2k*) and warm modes (equivalent or stronger AMOC with respect to *CTRL*).
 358 The three *oscillating simulations* behave in a similar way and will be described in more
 359 detail in the following sections.

360 During the cold modes (Figure 5, top), we observe strong consistency between the
 361 *oscillating simulations* and the *slow-recovery simulation*, to the point where it becomes

almost impossible to distinguish between them. These experiments show a maximum in atmospheric and oceanic cooling around 60° N (Figure 5*a, b*), where sea ice cover is now present both in winter and summer after the deep water formation sites vanished (Figure 5*c-e*). A second peak of winter sea ice is noticeable around 40° N, but is not as clear in summer sea ice nor mixed layer depth. This second peak corresponds to the closing of the warm water corridor off the western coast of Europe and the spread of winter sea ice in this region. It is around these latitudes that we observe a maximal reduction of the thermohaline circulation by up to 14 Sv (Figure 5*f*). Because of the loss of convection at high latitudes, the upper cell of the AMOC largely dwindles north and south of 20° N. The *warm simulations* follow a similar pattern of disruption, but are not nearly so intense. In *21.5k*, the soft decline of the AMOC is consistent with a shift southward of the convection sites, most likely resulting from a slightly cooler North Atlantic climate (Figure 5*c-f*). Summer sea ice extent is very similar to *CTRL* values in *21.5k*. The slowdown of the AMOC is slightly more pronounced in *21k*, with a clear reduction of sea surface temperature by as much as 2°C and of surface air temperature by up to 7.5°C at high latitudes (Figure 5*a, b* and *f*). It is remarkable that *21k*'s winter sea ice expansion and mixed layer depth shallowing are comparable to the *oscillating* and *slow-recovery* simulations, demonstrating an increased seasonality compared to the reference *CTRL* state (Figure 5*c-d*).

We do not observe such consistency between simulations during their warm modes (Figure 5, bottom). They all show a significant recovery from the cold modes, but it is impossible to underline a single common behaviour. For example, despite a couple of periodic recovery phases of the AMOC in *18.2k* (around 3,500, 7,000 and 9,000 years into the run; Figure 3*b*), the warm modes remain in a relatively cold-climate state (Figure 5*h-i*). At 60° N, sea surface temperatures are down 2°C and surface air temperatures drop by 6.5°C compared to *CTRL*. Shallower mixed layer depths around the same latitude indicate that Iceland/Irmingier Basin and Labrador Sea convection sites are still greatly disrupted (Figure 5*j*). This keeps the sea ice edge far south in both summer and winter (Figure 5*k-l*). On the other hand, the strong modes of the *warm simulations* are comparable to the reference *CTRL* state, only with a slightly cooler climate (Figure 5*i-j*) and a slower overturning circulation above 30° N in the Atlantic (Figure 5*m*). Amongst the *oscillating simulations*, the AMOC index is stronger than in *CTRL* (Figure 5*m*), increasing by as much as 2 Sv in the subpolar region. However, for the most part, these simulations also show disparities in key climate descriptors, at least in terms of amplitude of the anomalies. Surface temperatures and sea ice extent in *18.2k* and *17.8k* bear the closest resemblance across this subset of simulations, whereas temperatures and sea ice extent in *20.7k* and *19.4k* indicate a slightly warmer climate (Figure 5*h, i, j, l*) despite there being stronger ocean convection in *17.8k* (Figure 5*j*). The oscillating simulations all show an increase in winter sea ice around 40° N compared to *CTRL*, corresponding to the narrowing of the warm water corridor along the coast of western Europe (Figure 5*k*). In summary, none of the simulations exactly returned to the *CTRL* reference climate during their respective warm modes, indicating significant regional legacy induced by the imposed meltwater patterns.

5 Influence of the meltwater discharge

Abrupt climate changes are triggered by constant meltwater discharge in our simulations. Yet, we observe a strong non-linearity between the climate response and the location and the influx of freshwater, (Figure 3). For instance, despite a similar total influx of about 0.1 Sv, *19.4k* is tipped into an *oscillating* regime while *18.2k* ends up in a *slow-recovery* state. On the other hand, *20.7k* and *19.4k* display similar oscillating dynamics even though the total flux is around 20% weaker in *20.7k* than *19.4k*. All of this hints at the importance of differences in the meltwater discharge pattern. However, whilst the spatial distribution of freshwater forcing is comparable between *21k* and *20.7k*, only

414 *20.7k* manages to generate oscillations, demonstrating that while the spatial distribu-
 415 tion of the freshwater flux is an important control on the oceanic response, there is also
 416 a sweet spot in the perturbation conditions where the forcing needs to be strong enough
 417 to trigger a switch to stadial states, but not so strong that it (semi-)permanently sup-
 418 presses a recovery as in *18.2k*.

419 A threshold is reached in the cold climate modes, when the climate cools so far that
 420 it becomes insensitive to further meltwater discharge (Figure 5). Independent of the forc-
 421 ing, all simulations produce a similar spatial pattern in temperature, sea ice and deep
 422 water formation layout during the weak phases, but only when the surface atmosphere
 423 cools by as much as 15°C does the climate cross a tipping point where the cold phases
 424 can be sustained for a few hundred years. This corresponds to the vanishing of all oceanic
 425 convection north of 40° N (Figure 5c), resulting in an almost collapsed AMOC (up to
 426 12 Sv weaker) in the North Atlantic (Figure 5f). When all the deep water formation sites
 427 have vanished, the response becomes decoupled from the forcing and only smaller regional
 428 effects can be induced. This phenomenon resonates with the conclusion of Smith and Gre-
 429 gory (2009).

430 During warm AMOC modes, the differences in climate response seem to be driven
 431 by the regional patterns of discharge. The influence of the different forcings can be tracked
 432 by creating a composite of warm modes mixed layer depth anomalies (Figure S10), pro-
 433 ducing clearly distinct results from the *warm* simulations, the simulations with preva-
 434 lent North American meltwater inputs (*20.7k*, *19.4k*) and the simulations dominated by
 435 Arctic discharge (*18.2k*, *17.8k*). However, this relationship is sometimes counter-intuitive.
 436 For instance, despite having a stronger North American forcing in *19.4k* than in *18.2k*
 437 and *17.8k*, Labrador sea deep water formation is more impacted in the latter two sim-
 438 ulations. In addition, although *18.2k* and *17.8k* have high Arctic discharge, Iceland Sea
 439 convection intensifies and the Irminger Basin convection weakens.

440 The effect of Arctic/GIN Seas discharge is decisive for triggering the shift from warm
 441 to cold AMOC states and leads to the strongest modification of the warm modes (Fig-
 442 ure 5). The two most disrupted warm stages are found in *18.2k* and *17.8k*, both dom-
 443 inated by Arctic discharge. We infer that this comes from the relative position of other
 444 convection sites. For example, when released in the Arctic, freshwater follows the Green-
 445 land currents to reach the Irminger/Iceland basins relatively quickly, thus having under-
 446 gone less dispersal than if taking a longer more circuitous route, particularly compared
 447 to meltwater entrained in the Atlantic gyres (Born & Levermann, 2010). Arctic melt-
 448 water will thus target the main deep water formation sites without having been signif-
 449 icantly mixed into becoming warmer and saltier waters. Meltwater entering the GIN Seas
 450 should play a similar role, but the relatively low discharge in this area in our simulations
 451 makes it hard to conclude with certainty, and could explain why we do not observe a strong
 452 signal in this region (Figure S10).

453 Meltwater released off the northeast coast of North America have a weaker impact.
 454 Simulation *19.4k* has greater North Atlantic discharge, and similar fluxes to the Arctic
 455 and GIN Seas compared to *20.7k*. However, this increase in North Atlantic meltwater
 456 does not drive any significant ocean or climate response. Here, again, the explanation
 457 may relate to the location of the deep water formation sites. Because Labrador Sea con-
 458 vection is not always active, and easily shut down in our simulations, freshwater has to
 459 transit all around the subpolar gyre to target the more crucial sites in the eastern North
 460 Atlantic. By then, it has been mixed with tropical waters, weakening the forcing. The
 461 increased sensitivity to Arctic discharge compared to North American discharge in our
 462 simulations ties in with the conclusions of Roche et al. (2010) and Condrón and Win-
 463 sor (2012).

464 The existence of a sweet spot in the rate and location of meltwater discharge to the
 465 ocean for triggering climate transitions also depends on the background climate. Under-

standing the conditions leading to the creation of such a window of opportunity (Barker & Knorr, 2021) where abrupt climate changes can arise has been widely discussed (e.g. Brown & Galbraith, 2016; Zhang et al., 2017; Klockmann et al., 2018). Among the parameters likely to influence it, the choice of ice sheet reconstruction seems key, even more so in our simulations, as we rely on it both for the background climate state and for the meltwater forcing scenarios. In previous HadCM3-family deglaciation studies (e.g. Ivanovic et al., 2018; Gregoire et al., 2012), different ice sheets reconstructions did not yield as significant climate transitions, in spite of having a comparable baseline climate state (Kageyama et al., 2021) and magnitude of forcing. The higher temporal resolution of GLAC-1D and its treatment of the Eurasian ice sheet makes it a perfect candidate to attain this subtle balance, as hypothesised by Ivanovic et al. (2018). Precisely what about this particular reference state provides such a compliant framework for simulating AMOC oscillations may form the basis of future study, but we can reasonably hypothesise that very high-latitude meltwater is a pre-requisite for obtaining the sweet spot for producing climate variability, since without it, no oscillations are observed.

6 Bimodal warm states linked to reorganisation of deep water formation and subpolar gyre layout

Intriguingly, the *oscillating simulations* frequently undergo a double warm peak during times of strong AMOC (Figure 4b). This is particularly clear in the late cycles of *17.8k* (i.e. after 3,000 years), where the first peak in each warm phase is slightly cooler than the second. It indicates two distinct climate states separated by a cooling and then warming transition that is lower in amplitude than the cold-AMOC to warm-AMOC mode shift and which do not resemble the classical two-stage recovery hypothesis described by Renold et al. (2010) and Cheng et al. (2011). Changes in sites of deep water formation and the SubPolar Gyre (SPG) have been at the centre of recent studies of abrupt climate and ocean circulation changes (Li & Born, 2019; Klockmann et al., 2020) and could shed some light on this warm-mode transition stage. Hence, we next examine the relationship between the AMOC index, the longitude of the centre of Mass of the Mixed Layer Depth (MLD COM) and different physical indicators.

There is a linear relationship of roughly $1^{\circ}\text{C Sv}^{-1}$ between the AMOC index and the temperature at NGRIP (Figure 6a), demonstrating once again that AMOC index and NGRIP temperatures are interchangeable when it comes to identifying climate modes in our simulations. The intensity of the convection sites follow a similar trend (Figure 6b), with roughly a 10 metre increase of the maximum mixed layer depth in the North Atlantic for each degree of warming over Greenland. Both these relationships remain consistent irrespective of the specific warm modes that the *oscillating simulations* are in. However, for equivalent maximum AMOC strengths, the location of the deep water formation sites and the geometry of the subpolar gyre are clearly distinct between the two different warm modes. This is manifested in the ESPG index and latitude of the SPG COM, which split into two branches for high AMOC indices (Figure 6c-d). To further describe this phenomenon, we examine the winter and autumn convection layouts and sea ice formations for the two warm modes (Figure 7).

We follow the dynamics of the warm mode shifts by tracking the arrows in Figure 6, omitting in this analysis the initial spin-up period corresponding to values falling outside of the cycles (for example, the first 300 years in *20.7k*). Starting from a *cold* mode, the recovery of the AMOC is first fuelled by convection in the GIN Seas, with very little signal in the Irminger basin, which is covered in sea ice both in Autumn and Winter (Figure 7a, b, e, f). This results in a shift eastwards and northwards of the centre of mass of the convection sites, as indicated by a deeper mixed layer (Figure 6h). Although situated in an area of intense sea ice formation, the Labrador Sea deep water formation site is not always reactivated during this mode. As a result, the subpolar gyre, which is initially weak and contracted during the *cold* phase, gets slightly stronger and

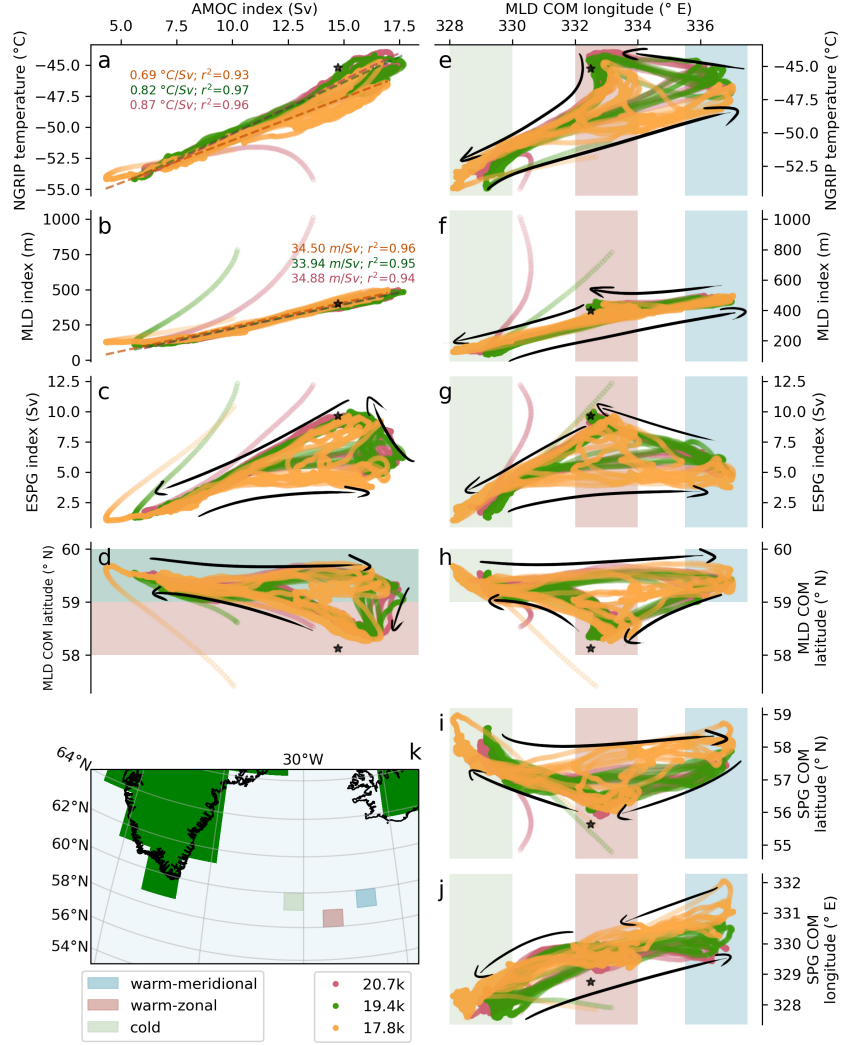


Figure 6. Phase plot of the three *oscillating simulations* showing the relationship between the maximal value of the overturning circulation in the Atlantic ocean at 26.5° N (AMOC index) and *a.* surface air temperature at NGRIP (42.32° W, 75.01° N), *b.* the maximum mixed layer depth in the Northern Hemisphere Atlantic (MLD index), *c.* the mean barotropic stream function in Eastern North Atlantic (ESPG index - see Klockmann et al. (2020) and Figure S9 for zones definition), *d.* the latitude of the centre of mass of the mixed layer depth (MLD COM latitude); and between the longitude of the centre of mass of the mixed layer depth (MLD COM longitude) and *e.* the temperature at NGRIP, *f.* the MLD index, *g.* the ESGP index, *h.* MLD COM latitude, *i.* the latitude of the centre of mass of the barotropic stream function in the subpolar region (SPG COM latitude) and *j.* the longitude of the centre of mass of the barotropic stream function in the subpolar region (SPG COM longitude). The calculation of the centre of mass is detailed in section S8. Colour shading indicates the location of the main areas of activity of the centre of mass of the mixed layer depth during the different modes, as plotted on panel *k.* Arrows indicate the direction of flow (through time) over the phase space; from green (cold) to blue (warm-meridional) to red (warm-zonal) modes. All time series were filtered following the algorithm presented in section S5. The black stars indicate the mean annual values calculated from the last 100-years of *CTRL*.

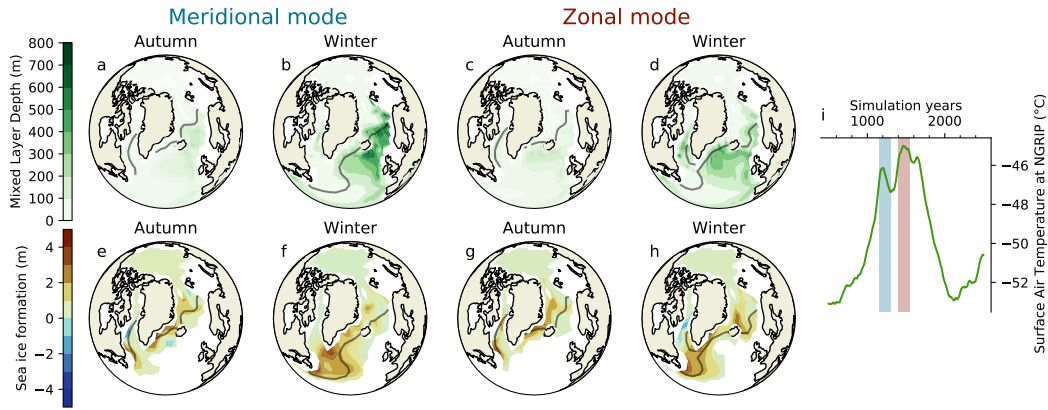


Figure 7. Seasonal Mixed layer depth (panels *a–d*) and sea ice formation (panels *e–h*) during the meridional (panels *a, b, e, f*) and zonal (panels *c, d, g, h*) warm modes in simulation *19.4k*, defined as the periods indicated in blue and red (respectively) in panel *i*. Autumn (September, October and November) and winter (December, January and February) seasonal means are shown for each variable in each of the two modes. Solid lines indicate the contour for 50% sea-ice concentration. Autumn sea ice formation is defined as the difference between November and September ice depth (in metres) and Winter between February and December. Panel *i* shows the times series of maximum Atlantic overturning circulation at 26° N in the same simulation, identifying the ‘meridional’ and ‘zonal’ modes.

518 extends eastwards (Figure 6*g, i, j*), entering the *warm-meridional* mode (so labelled for
 519 the disposition of the deep water formation sites during this phase). After sustaining a
 520 *warm-meridional* state for a few hundred years, the deep water formation layout is disrupted
 521 again to return to a state that resembles *CTRL* (comparing Figure 2 to Figure
 522 7*c–d*), with convection occurring primarily in the Iceland/Irminger basin and the resump-
 523 tion of Labrador Sea deep water formation in Autumn (Figure 7*c, d, g, h*). The convec-
 524 tion is distributed over a larger region and consequently the MLD index slightly dwindle.
 525 Conversely, the subpolar gyre intensifies, and moves southward and eastward (Fig-
 526 ure 6*i–j*). We call this state the *warm-zonal* phase.

527 Interestingly, we also observe short episodes of AMOC overshoot occurring immedi-
 528 ately after the transition from *cold* to *warm-meridional* modes. The overshoots only
 529 exist at the onset of *warm-meridional* modes and are associated with stronger convec-
 530 tion in the GIN Seas (characterised by a more eastern value of the MLD COM longitude
 531 in Figure 7*e*).

532 Overall, these two *warm* states of strong AMOC are different to the two modes de-
 533 scribed by Cheng et al. (2011), where there is a transfer of deep water formation across
 534 the Atlantic from the the Labrador Sea to the GIN Seas, the latter associated with an
 535 AMOC overshoot. In all three of *oscillating* simulations, a relatively strong convection
 536 is maintained throughout both warm phases of the cycle, and the deep water forma-
 537 tion layout only shifts around the Iceland basin.

538 7 A good example of Dansgaard-Oeschger events?

539 At first glance, the *oscillating simulations* resemble recorded D-O events. From a
 540 purely descriptive point of view, presented in Table 2, we observe a periodicity (defined
 541 as the inverse of the dominant frequency in Figure 4) of between 1,540 and 1,930 years

(the *18.2k* simulation has a periodicity of 1,290 years, but strictly we do not define this as an *oscillating* simulation). In terms of the duration of D-O cycles, this simulated periodicity is close to the range approximated from palaeo records (about 1,500 years) during times of regular occurrence (Thomas et al., 2009; Lohmann & Ditlevsen, 2019). As an example, we compared our simulated cycles with DO 9-11, which occurred between 44 ka BP and 40 ka BP (Figure 8). This is also very similar to the simulated events of Klockmann et al. (2020) and Armstrong et al. (2022), but two to three times longer than Peltier and Vettoretti (2014). As already discussed, *18.2k* does not qualify as an *oscillating* simulation due to its *slow-recovery* characteristics (section 4). Yet, in Figure 4, we observe two smaller peaks identified by the frequency analysis algorithm, one at $\sim 1,300$ years and one at $\sim 3,500$ years, which also correspond to typical D-O values (e.g. Kindler et al., 2014).

The temperature ranges between warm and cold climate/AMOC modes are similar, with changes of about 10°C recorded (Huber et al., 2006; Kindler et al., 2014) and simulated (this study) at NGRIP. From the other model studies cited in this study, only Peltier and Vettoretti (2014) obtained a similar amplitude of Greenland temperature change. Both Klockmann et al. (2020) and Armstrong et al. (2022) observed smaller transitions similar more to the 6°C amplitude of *18.2k* oscillations, but still within the lower range of reconstructed D-O events.

Our simulations also show a bipolar see-saw phenomenon (Stocker, 1998; Blunier & Brook, 2001), with a lag between the Northern and Southern Hemisphere temperature changes of around 100 years (Figure 8a-b), consistent with the suggestions of Blunier and Brook (2001) and Stocker and Johnsen (2003).

Notwithstanding these similarities with recorded D-O events, because all simulations were realised in a maximum glacial background (specifically, the LGM), the analogy between these simulations and D-O events is not straight forward. This is all the more true as we can also identify significant discrepancies between the model results and observations. For example, the simulated cycles do not match the typical shapes of D-O events (Lohmann & Ditlevsen, 2019); an abrupt warming followed by a slow cooling over a few hundred to a few thousand years within the warm phase followed by a sharper cooling to finish off the cycle. Our simulations displayed a gradual transition between the cold modes to the warm modes, and the strong-AMOC phases were maintained rather steadily for ~ 500 years before undergoing a slow cooling into the weak-AMOC phase of the cycle (Table 2). The warming and cooling rates are less sharp than palaeo-records suggest, with a typical rate of 3°C temperature change per 100 years, about 10 times slower than indicated in Lohmann and Ditlevsen (2019). It has to be noted that despite a potential damping of the warming and cooling rates due to the filtering, the duration of filtered signals matched the unfiltered ones well, indicating that our conclusion on the shape of the simulated cycles are not an artefact of the analytical method. Using the same model, but simulating an older time period, Armstrong et al. (2022) similarly produced an oscillating ocean/climate with warming rates not exceeding $3^{\circ}\text{C } 100\text{yrs}^{-1}$, in contrast to the ten times faster warming rates simulated by Peltier and Vettoretti (2014) and Klockmann et al. (2020) (their cooling rates overlap with ours).

Presently, we cannot categorically conclude whether or not our oscillations relate to D-O events. Differences in the shape of real and simulated D-O cycles may be explained by the quasi-idealised nature of our experiment design, specifically, the glacial maximum and fixed nature of our climate model boundary conditions/forcings (set to 21 ka, PMIP4 LGM protocol with GLAC-1D ice sheet plus the respective meltwater scenarios from the early deglaciation in GLAC-1D). The framework for our simulations was designed to simplify the identification of different behaviours in response to early deglacial meltwater forcing, mainly inspired by the hypotheses formed in conclusion to earlier work by Ivanovic et al. (2018). It provides a solid and systematic foundation for further work to study the mechanisms at play in the climate simulations presented here. However, this framework

Simulation	Periodicity (ka)	Amplitude ($^{\circ}\text{C}$)	Warming rate ($^{\circ}\text{C}100\text{yrs}^{-1}$)	Cooling rate ($^{\circ}\text{C}100\text{yrs}^{-1}$)
<i>20.7k</i>	1.54	10.9	4.94	-3.98
<i>19.4k</i>	1.93	8.92	5.19	-3.72
<i>18.2k</i>	1.29	5.90	2.84	-3.57
<i>17.8k</i>	1.67	7.65	4.17	-5.28
Peltier and Vettoretti (2014)	~ 0.8	~ 10	~ 50	~ -5
Klockmann et al. (2020)	1.5 to 2.0	5 to 6	25 to 50	-5 to -35
Armstrong et al. (2022)	~ 1.5	6.5 to 8.5	~ 3	~ -3

Table 2. Typical oscillation descriptors for the *oscillating* and *slow-recovery* simulations defined from the filtered NGRIP temperature time series (Figure 4) and compared to simulations from Peltier and Vettoretti (2014), Klockmann et al. (2020) and Armstrong et al. (2022). Periodicity was identified using the analysis presented in Figure 4c. Amplitude was defined as the difference between the warmest and coldest point of the filtered NGRIP temperature time series Figure 4b. Warming and cooling rates were defined as the maximum and minimum of the derivative of the filtered NGRIP temperatures time series, respectively. Descriptors of the simulations performed by Peltier and Vettoretti (2014) were estimated from Figure 1 by Vettoretti and Peltier (2018). Descriptors of the simulations performed by Klockmann et al. (2020) were taken from their main text. Descriptors of the simulations performed by Armstrong et al. (2022) were taken from the main text and estimated from Figure 2 by Armstrong et al. (2022).

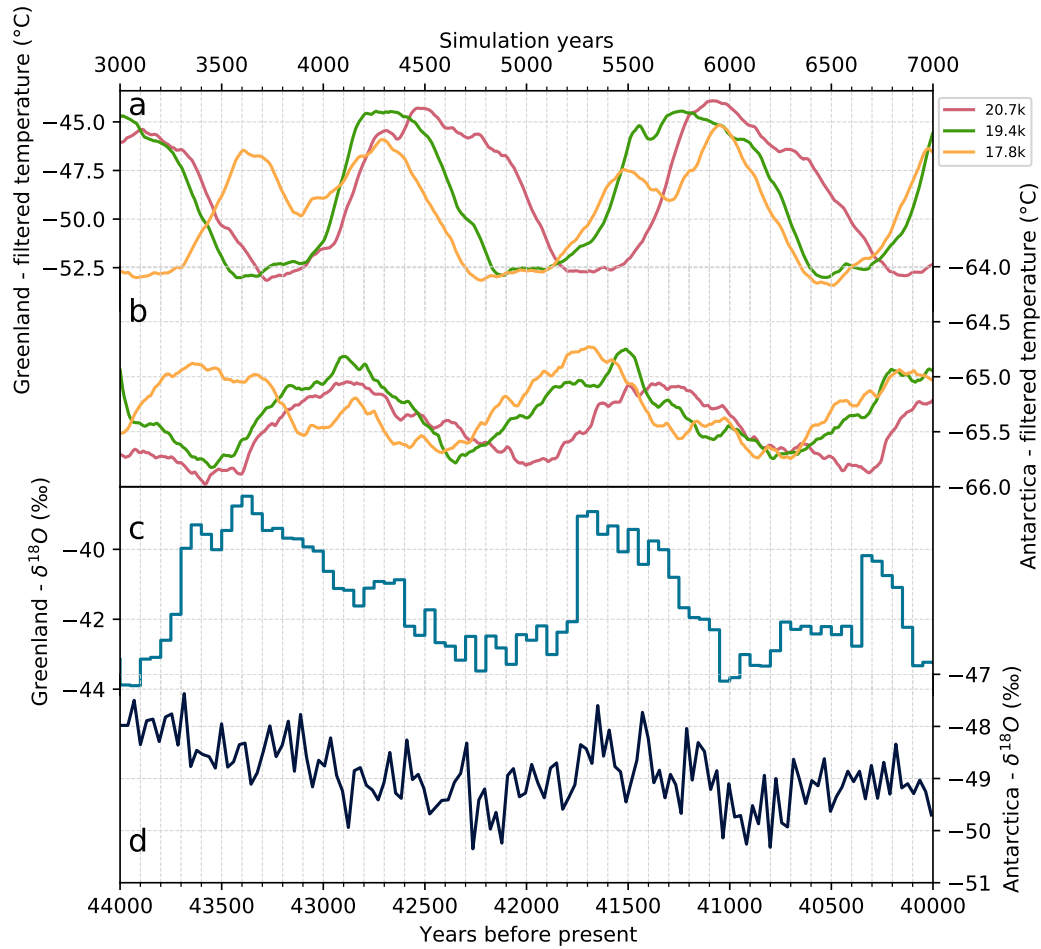


Figure 8. Temporally filtered signals of simulated surface air temperature over *a.* Greenland (NGRIP; 42.32° W, 75.01° N) and *b.* Antarctica (EPICA Dome C; 123.21° E, 75.06° S) for simulation years 3,000 to 7,000. *c.* NGRIP and *d.* EDML (Dronning Maud Land; 0.04° E, 75.00° S) $\delta^{18}O$ records between years 40,000 and 44,000 before present showing DO events 11, 10 and 9, from N.G.R.I.P (2004) and Barbante et al. (2006), respectively.

595 may interfere with or block some of the complex dynamics of D-O events and damp the
 596 abrupt climate changes. We indeed observe the sharpest cooling events at the onset of
 597 each simulation, indicating that the initial reorganisation of deep water formation sites
 598 in response to a change in freshwater forcing may lead to the strongest and fastest cli-
 599 mate disruption. Also, our setup does not include feedbacks between ice sheet melt and
 600 temperature changes, which could influence the periodicity of amplitude of changes (Gregoire
 601 et al., 2016; Ivanovic et al., 2017). We therefore speculate that implementing a transient
 602 meltwater pattern consistent with what is known about past ice sheets during times of
 603 abrupt climate change could be a good way to better account for the dynamical inter-
 604 actions and abrupt reorganisations of the earth system, but ultimately, transient cou-
 605 pled climate-ice sheet simulations are needed to fully unlock the challenge of understand-
 606 ing D-O cycles and abrupt deglacial climate change. Finally, the discrepancies between
 607 observed D-O cycles and our simulations may also be related to weaknesses in the cli-
 608 mate model itself. As concluded by Armstrong et al. (2022), this version of HadCM3 seems
 609 to be unable to capture the fast physics component that has been observed in (Vettoretti
 610 & Peltier, 2018), and this may be related to the representation of ocean vertical diffu-
 611 sion (Peltier & Vettoretti, 2014).

612 Furthermore, and specifically to address D-O cycles, we also need to be able to re-
 613 produce the phenomenon of oscillating weak-strong AMOC modes outside of a glacial
 614 maximum background. Marine Isotope Stage 3 (MIS3, 29–57 ka BP, (Lisiecki & Raymo,
 615 2005), as depicted in Figure 8c–d for comparison to our results, has been often consid-
 616 ered an appropriate candidate for such studies. Stadial conditions then were warmer than
 617 at the LGM, and it contains the most regular occurrences of D-O events recorded. Cur-
 618 rently, one major challenge for setting off such a suite of simulations is that our oscil-
 619 lations are triggered by meltwater discharge, with a strong dependency on nuanced dif-
 620 ferences in the rate and location of freshwater inputs to the ocean. Thus, robust and de-
 621 tailed constraints on ice sheet extent are necessary to design an appropriate model ex-
 622 periment.

623 Apart from Heinrich stadials, MIS3 was not a time when ice sheet melting is thought
 624 to have been particularly strong, and there is likely to have been a lower meltwater flux
 625 than in our *oscillating simulations* (Hughes et al., 2016; Batchelor et al., 2019). How-
 626 ever, DO 15-17 are believed to have been associated with changes of ice sheet extent (Lambeck,
 627 2004), and because their shape remarkably resembles the observed oscillatory cycles of
 628 our simulations (Barbante et al., 2006; Rasmussen et al., 2016; Erhardt et al., 2019), they
 629 could be good candidates for being triggered by relatively low-levels of Northern Hemi-
 630 sphere ice sheet melt; it is possible that a weaker glacial climate state had a more sen-
 631 sitive ocean to smaller meltwater fluxes than our LGM-based simulations. However, the
 632 further back in time we go, the less constrained ice sheet extent (and geometry more broadly)
 633 is, which again poses a practical limitation for how well such a climate model experiment
 634 could be designed to explore the detail of real past events. In any case, the next step in
 635 our investigation of the relationship between our simulations and real DO cycles will be
 636 to more deeply understand the physical mechanisms triggered during the model’s AMOC
 637 and Greenland temperature oscillations.

638 8 Conclusion

639 Using snapshots of the meltwater discharge derived from the GLAC-1D ice sheet
 640 history of the early last deglaciation, we produced a set of oscillating simulations in the
 641 HadCM3 climate model under glacial maximum (PMIP4 LGM) conditions. Switching
 642 regularly between cold and warm modes, this behaviour can only be attained in a nar-
 643 row range of circumstances: if the freshwater forcing is too strong and/or applied in a
 644 particularly sensitive part of the ocean, the climate cannot fully recover to a warm mode
 645 and stays cold for the majority of the simulation. On the other hand, if the forcing is

646 too weak, the transition to a cold mode is incomplete and the system rebounds to stay
647 permanently in a warm state.

648 Understanding what can be defined as a ‘weak’ or ‘strong’ freshwater flux is not
649 straightforward, as the response to the forcing is non-linear. All simulations are in the
650 range of plausible magnitudes for meltwater discharge over the last deglaciation — al-
651 though the scenarios are made quasi-idealised by sustaining a constant meltwater dis-
652 charge over thousands of years rather than following the transient history — but differ
653 significantly in terms of total amplitude, and the geographical distribution of the fresh-
654 water fluxes. We identified the release regions closest to the main convection sites, namely
655 the Nordic Seas and the Irminger/Iceland Basins, to be the most sensitive regions to melt-
656 water forcing. One possible inference from this finding is that in spite of being smaller
657 in size compared to the North American ice sheet, Eurasian ice sheet demise punches
658 above its weight in having the potential to trigger abrupt climate changes over the last
659 deglaciation. Conversely, Laurentide ice sheet meltwater is required to be much more sub-
660 stantial to produce similar disruptions to Atlantic Ocean circulation and climate. The
661 impact of the initial climate and ocean state on our results must also be considered. The
662 cold interstadial state obtained with GLAC-1D ice sheets, with a relatively weak AMOC,
663 convection concentrated around Iceland and extensive sea ice in the Western North At-
664 lantic, creates a background that may favour the triggering of abrupt climate changes
665 from Eurasian ice sheet melting.

666 When reaching a cold mode in our simulations, the ocean and climate response to
667 meltwater forcing becomes decoupled from the direct influence of freshwater input at high
668 latitudes. Because the AMOC is collapsed in these states, and the susceptible North At-
669 lantic deep water formation sites vanished, meltwater perturbations will not propagate
670 any longer, producing only smaller, regional perturbations. Cold modes correspond to
671 an extreme cooling of the North Atlantic, most brutally over former convection regions,
672 with winter sea ice stretching down to Spain. We note a strong consistency in the cli-
673 mate change pattern of all simulations irrespective of whether they belong to the *oscil-*
674 *lating*, *slow-recovery*, or, to a lesser extent, *warm* clusters of simulations. This is not true
675 for the warm modes, where the response is very dependent on the meltwater forcing sce-
676 nario. We observe a range of different AMOC responses, from overshooting to damping,
677 and the resulting climate is very different for each of the simulations. In particular, the
678 simulations dominated by Arctic discharge never manage to completely return to the ref-
679 erence (*CTRL*) state. We also observe a two-phase, bi-modal warm condition in the *os-*
680 *cillating* simulations, with shifts between deep water-formation sites from a more merid-
681 ional distribution (with primary convection situated in the Nordic seas) to a more zonal
682 configuration comparable to *CTRL*. Resumption of Labrador Sea convection is incon-
683 sistent, sometimes being short lived and intense and sometimes being wholly absent, and
684 in these glacial simulations, its connection to the upper cell of the overturning circula-
685 tion is tenuous.

686 In summary, while we cannot conclusively determine that the oscillations we sim-
687 ulate are comparable to D-O events, there are resemblances that make such a compar-
688 ison inviting. D-O events were rarely observed in full-glacial climates and are not believed
689 to be directly forced by changes in ice sheet meltwater discharge. Still, the oscillating
690 simulations presented here offer a valuable framework to analyse further the mechanisms
691 behind the millennial-scale variability in glacial backgrounds. Intriguingly, they provide
692 a set of insightful simulations that are so far unique in that relatively small influxes of
693 freshwater trigger self-sustaining AMOC and Greenland temperature oscillations from
694 glacial *maximum* conditions with a very large LGM North American ice sheet. Finally,
695 the presented simulations pave the way for further study of ice sheet meltwater as a *trig-*
696 *ger*, but not a direct *driver*, of abrupt climate changes within the last deglaciation.

697 9 Data and code availability

698 The new model data presented here will be available from the University of Leeds
699 Research Data repository upon acceptance of the article. The presented plots realised
700 were produced using the matplotlib python library and some of the colormaps were taken
701 from Crameri et al. (2020). The code is available on github at [https://github.com/
702 Olnavy/ROME2022_paleoceanography_oscillations](https://github.com/Olnavy/ROME2022_paleoceanography_oscillations), it relies on the packages *pyleao-
703 clim_leeds v1.0* (https://github.com/Olnavy/pylaeoclim_leeds) and *mw_protocol v1.0*
704 (https://github.com/climate-ice/mw_protocol), also created by the main author.

705 Acknowledgments

706 YMR was supported by the Leeds-York-Hull Natural Environment Research Coun-
707 cil (NERC) Doctoral Training Partnership (DTP) Panorama under grant NE/S007458/1.
708 LJG was funded by MR/S016961/1 and SST was funded by NE/T007443/1. Simulations
709 were run on the high performance facilities ARC3 and ARC4 at the University of Leeds,
710 UK. All climate and ocean circulation proxy data and model simulations compared to
711 are published elsewhere, with the exception of Armstrong et al. 2022, which is still un-
712 der review. Thanks are due to CEMAC for technical assistance on the numerical resource,
713 with special thanks to Richard Rigby for assistance with the scripts for managing and
714 processing model output. Thanks to Julia Tindal and Steve Hunter for helpful techni-
715 cal discussions and investigations. Thanks to Kerim Nisancioglu and Chuncheng Guo
716 for insightful discussion about the paper, and to Heather Andres whose presentation at
717 vEGU21 inspired Figure 6.

References

- 718
- 719 Abe-Ouchi, A., Saito, F., Kageyama, M., Braconnot, P., Harrison, S. P., Lam-
720 beck, K., ... Takahashi, K. (2015, November). Ice-sheet configuration
721 in the CMIP5/PMIP3 Last Glacial Maximum experiments. *Geoscientific Model Development*, 8(11), 3621–3637. Retrieved 2020-03-04, from
722 <https://www.geosci-model-dev.net/8/3621/2015/> (Publisher: Copernicus
723 GmbH) doi: <https://doi.org/10.5194/gmd-8-3621-2015>
- 724
- 725 Argus, D. F., Peltier, W. R., Drummond, R., & Moore, A. W. (2014, July). The
726 Antarctica component of postglacial rebound model ICE-6G.c (VM5a) based
727 on GPS positioning, exposure age dating of ice thicknesses, and relative sea
728 level histories. *Geophysical Journal International*, 198(1), 537–563. Retrieved
729 2020-03-15, from [https://academic.oup.com/gji/article/198/1/537/
730 2874192](https://academic.oup.com/gji/article/198/1/537/2874192) (Publisher: Oxford Academic) doi: 10.1093/gji/ggu140
- 731
- 732 Barbante, C., Barnola, J.-M., Becagli, S., Beer, J., Bigler, M., Boutron, C., ...
733 EPICA Community Members (2006, November). One-to-one coupling of
734 glacial climate variability in Greenland and Antarctica. *Nature*, 444(7116).
735 Retrieved 2021-12-20, from <https://www.nature.com/articles/nature05301>
736 doi: 10.1038/nature05301
- 737
- 738 Barker, S., Chen, J., Gong, X., Jonkers, L., Knorr, G., & Thornalley, D. (2015,
739 April). Icebergs not the trigger for North Atlantic cold events. *Nature*,
740 520(7547), 333–336. Retrieved 2019-05-29, from [https://www.nature.com/
741 articles/nature14330](https://www.nature.com/articles/nature14330) doi: 10.1038/nature14330
- 742
- 743 Barker, S., & Knorr, G. (2021, April). Millennial scale feedbacks determine the
744 shape and rapidity of glacial termination. *Nature Communications*, 12(1),
745 2273. Retrieved 2021-09-10, from [https://www.nature.com/articles/
746 s41467-021-22388-6](https://www.nature.com/articles/s41467-021-22388-6) doi: 10.1038/s41467-021-22388-6
- 747
- 748 Batchelor, C. L., Margold, M., Krapp, M., Murton, D. K., Dalton, A. S., Gibbard,
749 P. L., ... Manica, A. (2019, August). The configuration of Northern Hemi-
750 sphere ice sheets through the Quaternary. *Nature Communications*, 10(1),
751 1–10. Retrieved 2019-09-20, from [https://www.nature.com/articles/
752 s41467-019-11601-2](https://www.nature.com/articles/s41467-019-11601-2) doi: 10.1038/s41467-019-11601-2
- 753
- 754 Beghin, P., Charbit, S., Dumas, C., Kageyama, M., & Ritz, C. (2015, October).
755 How might the North American ice sheet influence the northwestern Eurasian
756 climate? *Climate of the Past*, 11(10), 1467–1490. Retrieved 2021-09-08,
757 from <https://cp.copernicus.org/articles/11/1467/2015/> (Publisher:
758 Copernicus GmbH) doi: 10.5194/cp-11-1467-2015
- 759
- 760 Bereiter, B., Eggleston, S., Schmitt, J., Nehrbass-Ahles, C., Stocker, T. F., Fis-
761 cher, H., ... Chappellaz, J. (2015). Revision of the EPICA Dome C
762 CO₂ record from 800 to 600 kyr before present. *Geophysical Research
763 Letters*, 42(2), 542–549. Retrieved 2020-03-10, from [https://agupubs.
764 onlinelibrary.wiley.com/doi/abs/10.1002/2014GL061957](https://agupubs.onlinelibrary.wiley.com/doi/abs/10.1002/2014GL061957) (eprint:
765 <https://agupubs.onlinelibrary.wiley.com/doi/pdf/10.1002/2014GL061957>) doi:
766 10.1002/2014GL061957
- 767
- 768 Berger, A. (1978, December). Long-Term Variations of Daily Insolation and Qua-
769 ternary Climatic Changes. *Journal of the Atmospheric Sciences*, 35(12),
770 2362–2367. Retrieved 2020-03-10, from [https://journals.ametsoc.org/doi/
771 abs/10.1175/1520-0469%281978%29035%3C2362%3ALTVOI%3E2.0.CO%3B2](https://journals.ametsoc.org/doi/abs/10.1175/1520-0469%281978%29035%3C2362%3ALTVOI%3E2.0.CO%3B2)
772 (Publisher: American Meteorological Society) doi: 10.1175/1520-0469(1978)
035<2362:LTVOI>2.0.CO;2
- 773
- 774 Bethke, I., Li, C., & Nisancioglu, K. H. (2012). Can we use ice sheet re-
775 constructions to constrain meltwater for deglacial simulations? *Paleo-
776 oceanography*, 27(2). Retrieved 2020-03-10, from [https://agupubs.
777 onlinelibrary.wiley.com/doi/abs/10.1029/2011PA002258](https://agupubs.onlinelibrary.wiley.com/doi/abs/10.1029/2011PA002258) (eprint:
778 <https://agupubs.onlinelibrary.wiley.com/doi/pdf/10.1029/2011PA002258>) doi:
779 10.1029/2011PA002258

- 773 Bigg, G. R., & Wadley, M. R. (2001). Millennial-scale variability in the oceans:
774 an ocean modelling view. *Journal of Quaternary Science*, 16(4), 309–319.
775 Retrieved 2021-09-06, from [https://onlinelibrary.wiley.com/doi/abs/](https://onlinelibrary.wiley.com/doi/abs/10.1002/jqs.599)
776 10.1002/jqs.599 doi: 10.1002/jqs.599
- 777 Blunier, T., & Brook, E. J. (2001, January). Timing of Millennial-Scale Cli-
778 mate Change in Antarctica and Greenland During the Last Glacial Pe-
779 riod. *Science*, 291(5501), 109–112. Retrieved 2020-02-26, from [https://](https://science.sciencemag.org/content/291/5501/109)
780 science.sciencemag.org/content/291/5501/109 (Publisher: Ameri-
781 can Association for the Advancement of Science Section: Report) doi:
782 10.1126/science.291.5501.109
- 783 Bond, G., Broecker, W., Johnsen, S., McManus, J., Labeyrie, L., Jouzel, J., & Bo-
784 nani, G. (1993, September). Correlations between climate records from North
785 Atlantic sediments and Greenland ice. *Nature*, 365(6442), 143–147. Retrieved
786 2020-02-26, from <https://www.nature.com/articles/365143a0> (Number:
787 6442 Publisher: Nature Publishing Group) doi: 10.1038/365143a0
- 788 Born, A., & Levermann, A. (2010). The 8.2 ka event: Abrupt transition of
789 the subpolar gyre toward a modern North Atlantic circulation. *Geo-*
790 *chemistry, Geophysics, Geosystems*, 11(6). Retrieved 2019-09-13, from
791 [https://agupubs.pericles-prod.literatumonline.com/doi/abs/10.1029/](https://agupubs.pericles-prod.literatumonline.com/doi/abs/10.1029/2009GC003024)
792 2009GC003024 doi: 10.1029/2009GC003024
- 793 Braconnot, P., Otto-Bliesner, B., Harrison, S., Joussaume, S., Peterchmitt, J.-Y.,
794 Abe-Ouchi, A., ... Zhao, Y. (2007, June). Results of PMIP2 coupled sim-
795 ulations of the Mid-Holocene and Last Glacial Maximum – Part 2:
796 feedbacks with emphasis on the location of the ITCZ and mid- and high lati-
797 tudes heat budget. *Climate of the Past*, 3(2), 279–296. Retrieved 2022-02-02,
798 from <https://cp.copernicus.org/articles/3/279/2007/> (Publisher:
799 Copernicus GmbH) doi: 10.5194/cp-3-279-2007
- 800 Bradwell, T., Small, D., Fabel, D., Clark, C. D., Chiverrell, R. C., Saher, M. H.,
801 ... Cofaigh, C. O. (2021). Pattern, style and timing of British–Irish
802 Ice Sheet retreat: Shetland and northern North Sea sector. *Journal*
803 *of Quaternary Science*, 36(5), 681–722. Retrieved 2021-09-07, from
804 <https://onlinelibrary.wiley.com/doi/abs/10.1002/jqs.3163> (eprint:
805 <https://onlinelibrary.wiley.com/doi/pdf/10.1002/jqs.3163>) doi: 10.1002/
806 jqs.3163
- 807 Briggs, R. D., Pollard, D., & Tarasov, L. (2014, November). A data-constrained
808 large ensemble analysis of Antarctic evolution since the Eemian. *Quater-*
809 *nary Science Reviews*, 103, 91–115. Retrieved 2020-03-08, from [http://](http://www.sciencedirect.com/science/article/pii/S0277379114003448)
810 www.sciencedirect.com/science/article/pii/S0277379114003448 doi:
811 10.1016/j.quascirev.2014.09.003
- 812 Broecker, W. S., Peteet, D. M., & Rind, D. (1985, May). Does the
813 ocean–atmosphere system have more than one stable mode of operation? *Na-*
814 *ture*, 315(6014), 21–26. Retrieved 2020-03-04, from [https://www.nature.com/](https://www.nature.com/articles/315021a0)
815 [articles/315021a0](https://www.nature.com/articles/315021a0) (Number: 6014 Publisher: Nature Publishing Group)
816 doi: 10.1038/315021a0
- 817 Brown, N., & Galbraith, E. (2016, August). Hosed vs. unhosed: Interruptions of
818 the Atlantic Meridional Overturning Circulation in a global coupled model,
819 with and without freshwater forcing. *Climate of the Past*, 12, 1663–1679. doi:
820 10.5194/cp-12-1663-2016
- 821 Bryan, K., & Cox, M. D. (1972, October). An Approximate Equation of State for
822 Numerical Models of Ocean Circulation. *Journal of Physical Oceanography*,
823 2(4), 510–514. Retrieved 2021-09-07, from [https://journals.ametsoc.org/](https://journals.ametsoc.org/view/journals/phoc/2/4/1520-0485_1972_002_0510_aaeosf_2_0_co_2.xml)
824 [view/journals/phoc/2/4/1520-0485_1972_002_0510_aaeosf_2_0_co_2.xml](https://journals/phoc/2/4/1520-0485_1972_002_0510_aaeosf_2_0_co_2.xml)
825 doi: 10.1175/1520-0485(1972)002<0510:AAEOSF>2.0.CO;2
- 826 Burckel, P., Waelbroeck, C., Gherardi, J. M., Pichat, S., Arz, H., Lippold, J., ...
827 Thil, F. (2015). Atlantic Ocean circulation changes preceded millennial

- 828 tropical South America rainfall events during the last glacial. *Geophysical Re-*
829 *search Letters*, 42(2), 411–418. Retrieved 2020-03-04, from [https://agupubs](https://agupubs.onlinelibrary.wiley.com/doi/abs/10.1002/2014GL062512)
830 [.onlinelibrary.wiley.com/doi/abs/10.1002/2014GL062512](https://agupubs.onlinelibrary.wiley.com/doi/abs/10.1002/2014GL062512) (eprint:
831 <https://agupubs.onlinelibrary.wiley.com/doi/pdf/10.1002/2014GL062512>) doi:
832 10.1002/2014GL062512
- 833 Böhm, E., Lippold, J., Gutjahr, M., Frank, M., Blaser, P., Antz, B., ... Deininger,
834 M. (2015, January). Strong and deep Atlantic meridional overturning cir-
835 culation during the last glacial cycle. *Nature*, 517(7532), 73–76. Retrieved
836 2019-09-20, from <https://www.nature.com/articles/nature14059> doi:
837 10.1038/nature14059
- 838 Cheng, J., Liu, Z., He, F., L. Otto-Bliesner, B., Brady, E., & Wehrenberg, M. (2011,
839 January). Simulated Two-Stage Recovery of Atlantic Meridional Overturning
840 Circulation During the Last Deglaciation. *Abrupt Climate Change: Mecha-*
841 *nisms, Patterns, and Impacts*, 193, 75–92. doi: 10.1029/2010gm001014
- 842 Clark, P. U., Dyke, A. S., Shakun, J. D., Carlson, A. E., Clark, J., Wohlfarth,
843 B., ... McCabe, A. M. (2009, August). The Last Glacial Maximum.
844 *Science*, 325(5941), 710–714. Retrieved 2020-03-08, from [https://](https://science.sciencemag.org/content/325/5941/710)
845 science.sciencemag.org/content/325/5941/710 (Publisher: American
846 Association for the Advancement of Science Section: Research Article) doi:
847 10.1126/science.1172873
- 848 Clark, P. U., Pisias, N. G., Stocker, T. F., & Weaver, A. J. (2002, February).
849 The role of the thermohaline circulation in abrupt climate change. *Nature*,
850 415(6874), 863–869. Retrieved 2020-03-04, from [https://www.nature.com/](https://www.nature.com/articles/415863a)
851 [articles/415863a](https://www.nature.com/articles/415863a) (Number: 6874 Publisher: Nature Publishing Group) doi:
852 10.1038/415863a
- 853 Condron, A., & Winsor, P. (2012, December). Meltwater routing and the Younger
854 Dryas. *Proceedings of the National Academy of Sciences*, 109(49), 19928–
855 19933. Retrieved 2020-07-15, from [http://www.pnas.org/cgi/doi/10.1073/](http://www.pnas.org/cgi/doi/10.1073/pnas.1207381109)
856 [pnas.1207381109](http://www.pnas.org/cgi/doi/10.1073/pnas.1207381109) doi: 10.1073/pnas.1207381109
- 857 Cox, P. (2001, January). Description of the TRIFFID dynamic global vegetation
858 model. *Hadley Centre Technical Note*, 24.
- 859 Cox, P. M., Betts, R. A., Bunton, C. B., Essery, R. L. H., Rowntree, P. R., &
860 Smith, J. (1999, March). The impact of new land surface physics on the GCM
861 simulation of climate and climate sensitivity. *Climate Dynamics*, 15(3), 183–
862 203. Retrieved 2020-07-09, from <https://doi.org/10.1007/s003820050276>
863 doi: 10.1007/s003820050276
- 864 Crameri, F., Shephard, G. E., & Heron, P. J. (2020, October). The misuse
865 of colour in science communication. *Nature Communications*, 11(1),
866 5444. Retrieved 2022-03-18, from [https://www.nature.com/articles/](https://www.nature.com/articles/s41467-020-19160-7)
867 [s41467-020-19160-7](https://www.nature.com/articles/s41467-020-19160-7) (Number: 1 Publisher: Nature Publishing Group) doi:
868 10.1038/s41467-020-19160-7
- 869 Dansgaard, W., Johnsen, S. J., Clausen, H. B., Dahl-Jensen, D., Gundestrup, N. S.,
870 Hammer, C. U., ... Bond, G. (1993, July). Evidence for general instability
871 of past climate from a 250-kyr ice-core record. *Nature*, 364(6434), 218–220.
872 Retrieved 2019-09-16, from <https://www.nature.com/articles/364218a0>
873 doi: 10.1038/364218a0
- 874 Davies-Barnard, T., Ridgwell, A., Singarayer, J., & Valdes, P. (2017, October).
875 Quantifying the influence of the terrestrial biosphere on glacial–interglacial cli-
876 mate dynamics. *Climate of the Past*, 13(10), 1381–1401. Retrieved 2022-03-01,
877 from <https://cp.copernicus.org/articles/13/1381/2017/> (Publisher:
878 Copernicus GmbH) doi: 10.5194/cp-13-1381-2017
- 879 Dentith, J. E., Ivanovic, R. F., Gregoire, L. J., Tindall, J. C., & Smith, R. S. (2019,
880 February). Ocean circulation drifts in multi-millennial climate simulations:
881 the role of salinity corrections and climate feedbacks. *Climate Dynamics*,
882 52(3), 1761–1781. Retrieved 2021-10-28, from <https://doi.org/10.1007/>

- 883 s00382-018-4243-y doi: 10.1007/s00382-018-4243-y
- 884 Denton, G. H., Broecker, W. S., & Alley, R. B. (2006, August). The mystery interval
885 17.5 to 14.5 kyrs ago. *PAGES news*, 14(2), 14–16. Retrieved 2020-07-15, from
886 <http://www.pastglobalchanges.org/products/12189> doi: 10.22498/pages
887 .14.2.14
- 888 Dokken, T. M., Nisancioglu, K. H., Li, C., Battisti, D. S., & Kissel, C. (2013).
889 Dansgaard-Oeschger cycles: Interactions between ocean and sea ice intrinsic to
890 the Nordic seas. *Paleoceanography*, 28(3), 491–502. Retrieved 2019-09-20, from
891 <https://agupubs.onlinelibrary.wiley.com/doi/abs/10.1002/palo.20042>
892 doi: 10.1002/palo.20042
- 893 Du, J., Haley, B. A., & Mix, A. C. (2020, August). Evolution of the Global Over-
894 turning Circulation since the Last Glacial Maximum based on marine au-
895 thigenic neodymium isotopes. *Quaternary Science Reviews*, 241, 106396.
896 Retrieved 2022-02-02, from [https://www.sciencedirect.com/science/
897 article/pii/S0277379120303589](https://www.sciencedirect.com/science/article/pii/S0277379120303589) doi: 10.1016/j.quascirev.2020.106396
- 898 Dyke, A. (2004, January). An outline of North American deglaciation with empha-
899 sis on central and northern Canada. *Developments in Quaternary Sciences*,
900 2, 373–424. Retrieved 2021-04-05, from [https://www.sciencedirect.com/
901 science/article/pii/S1571086604802094](https://www.sciencedirect.com/science/article/pii/S1571086604802094) (Publisher: Elsevier) doi:
902 10.1016/S1571-0866(04)80209-4
- 903 Erhardt, T., Capron, E., Rasmussen, S. O., Schüpbach, S., Bigler, M., Adolphi,
904 F., & Fischer, H. (2019, April). Decadal-scale progression of the onset of
905 Dansgaard–Oeschger warming events. *Climate of the Past*, 15(2), 811–825.
906 Retrieved 2021-12-20, from [https://cp.copernicus.org/articles/15/811/
907 2019/](https://cp.copernicus.org/articles/15/811/2019/) (Publisher: Copernicus GmbH) doi: 10.5194/cp-15-811-2019
- 908 Fletcher, W. J., Sánchez Goñi, M. F., Allen, J. R. M., Cheddadi, R., Combourieu-
909 Nebout, N., Huntley, B., ... Tzedakis, P. C. (2010, October). Millennial-
910 scale variability during the last glacial in vegetation records from Eu-
911 rope. *Quaternary Science Reviews*, 29(21), 2839–2864. Retrieved 2021-
912 09-06, from [https://www.sciencedirect.com/science/article/pii/
913 S0277379109003886](https://www.sciencedirect.com/science/article/pii/S0277379109003886) doi: 10.1016/j.quascirev.2009.11.015
- 914 Fofonoff, N. P. (1985). Physical properties of seawater: A new salinity scale
915 and equation of state for seawater. *Journal of Geophysical Research:
916 Oceans*, 90(C2), 3332–3342. Retrieved 2021-09-07, from [https://agupubs
917 .onlinelibrary.wiley.com/doi/abs/10.1029/JC090iC02p03332](https://agupubs.onlinelibrary.wiley.com/doi/abs/10.1029/JC090iC02p03332) doi:
918 10.1029/JC090iC02p03332
- 919 Fofonoff, N. P., & Millard Jr, R. C. (1983). Algorithms for the computation of
920 fundamental properties of seawater. *UNESCO Technical Papers in Marine Sci-
921 ences*. Retrieved 2021-09-07, from [https://repository.oceanbestpractices
922 .org/handle/11329/109](https://repository.oceanbestpractices.org/handle/11329/109) doi: 10.25607/OBP-1450
- 923 Ganopolski, A., & Rahmstorf, S. (2001, January). Rapid changes of glacial cli-
924 mate simulated in a coupled climate model. *Nature*, 409(6817), 153–158. Re-
925 trieved 2019-09-19, from <https://www.nature.com/articles/35051500> doi:
926 10.1038/35051500
- 927 Gebbie, G. (2014). How much did Glacial North Atlantic Water shoal? *Paleo-
928 ceanography*, 29(3), 190–209. Retrieved 2021-09-08, from [https://agupubs
929 .onlinelibrary.wiley.com/doi/abs/10.1002/2013PA002557](https://agupubs.onlinelibrary.wiley.com/doi/abs/10.1002/2013PA002557) (eprint:
930 <https://agupubs.onlinelibrary.wiley.com/doi/pdf/10.1002/2013PA002557>) doi:
931 10.1002/2013PA002557
- 932 Gordon, C., Cooper, C., Senior, C. A., Banks, H., Gregory, J. M., Johns, T. C.,
933 ... Wood, R. A. (2000, February). The simulation of SST, sea ice ex-
934 tents and ocean heat transports in a version of the Hadley Centre coupled
935 model without flux adjustments. *Climate Dynamics*, 16(2), 147–168. Re-
936 trieved 2020-07-09, from <https://doi.org/10.1007/s003820050010> doi:
937 10.1007/s003820050010

- 938 Goñi, M. F. S., Turon, J.-L., Eynaud, F., & Gendreau, S. (2000, November). Euro-
 939 pean Climatic Response to Millennial-Scale Changes in the Atmosphere–Ocean
 940 System during the Last Glacial Period. *Quaternary Research*, 54(3), 394–403.
 941 Retrieved 2021-10-26, from [https://www.cambridge.org/core/journals/
 942 quaternary-research/article/abs/european-climatic-response-to
 943 -millennialscale-changes-in-the-atmosphereocean-system-during-the
 944 -last-glacial-period/576DB6EF96D6923ED701B117C5939CD0#access-block](https://www.cambridge.org/core/journals/quaternary-research/article/abs/european-climatic-response-to-millennialscale-changes-in-the-atmosphereocean-system-during-the-last-glacial-period/576DB6EF96D6923ED701B117C5939CD0#access-block)
 945 (Publisher: Cambridge University Press) doi: 10.1006/qres.2000.2176
- 946 Gregoire, L. J., Ivanovic, R. F., Maycock, A. C., Valdes, P. J., & Stevenson, S.
 947 (2018, November). Holocene lowering of the Laurentide ice sheet affects North
 948 Atlantic gyre circulation and climate. *Climate Dynamics*, 51(9), 3797–3813.
 949 Retrieved 2021-02-16, from <https://doi.org/10.1007/s00382-018-4111-9>
 950 doi: 10.1007/s00382-018-4111-9
- 951 Gregoire, L. J., Otto-Bliesner, B., Valdes, P. J., & Ivanovic, R. (2016).
 952 Abrupt Bølling warming and ice saddle collapse contributions to the
 953 Meltwater Pulse 1a rapid sea level rise. *Geophysical Research Let-
 954 ters*, 43(17), 9130–9137. Retrieved 2022-03-04, from [https://
 955 onlinelibrary.wiley.com/doi/abs/10.1002/2016GL070356](https://onlinelibrary.wiley.com/doi/abs/10.1002/2016GL070356) (eprint:
 956 <https://onlinelibrary.wiley.com/doi/pdf/10.1002/2016GL070356>) doi:
 957 10.1002/2016GL070356
- 958 Gregoire, L. J., Payne, A. J., & Valdes, P. J. (2012, July). Deglacial rapid sea
 959 level rises caused by ice-sheet saddle collapses. *Nature*, 487(7406), 219–
 960 222. Retrieved 2020-03-15, from [https://www.nature.com/articles/
 961 nature11257](https://www.nature.com/articles/nature11257) (Number: 7406 Publisher: Nature Publishing Group) doi:
 962 10.1038/nature11257
- 963 Gregoire, L. J., Valdes, P. J., & Payne, A. J. (2015). The rela-
 964 tive contribution of orbital forcing and greenhouse gases to the
 965 North American deglaciation. *Geophysical Research Letters*,
 966 42(22), 9970–9979. Retrieved 2020-03-16, from [https://agupubs
 967 .onlinelibrary.wiley.com/doi/abs/10.1002/2015GL066005](https://agupubs.onlinelibrary.wiley.com/doi/abs/10.1002/2015GL066005) (eprint:
 968 <https://agupubs.onlinelibrary.wiley.com/doi/pdf/10.1002/2015GL066005>) doi:
 969 10.1002/2015GL066005
- 970 Guo, C., Nisancioglu, K. H., Bentsen, M., Bethke, I., & Zhang, Z. (2019,
 971 June). Equilibrium simulations of Marine Isotope Stage 3 climate. *Cli-
 972 mate of the Past*, 15(3), 1133–1151. Retrieved 2020-05-11, from [https://
 973 www.clim-past.net/15/1133/2019/](https://www.clim-past.net/15/1133/2019/) (Publisher: Copernicus GmbH) doi:
 974 <https://doi.org/10.5194/cp-15-1133-2019>
- 975 Heinrich, H. (1988, March). Origin and consequences of cyclic ice rafting in the
 976 Northeast Atlantic Ocean during the past 130,000 years. *Quaternary Research*,
 977 29(2), 142–152. Retrieved 2019-09-16, from [http://www.sciencedirect.com/
 978 science/article/pii/0033589488900579](http://www.sciencedirect.com/science/article/pii/0033589488900579) doi: 10.1016/0033-5894(88)90057-
 979 9
- 980 Hemming, S. R. (2004, March). Heinrich events: Massive late Pleistocene detritus
 981 layers of the North Atlantic and their global climate imprint. *Reviews of Geo-
 982 physics*, 42(1). Retrieved 2019-08-27, from [https://agupubs.onlinelibrary
 983 .wiley.com/doi/full/10.1029/2003RG000128](https://agupubs.onlinelibrary.wiley.com/doi/full/10.1029/2003RG000128) doi: 10.1029/2003RG000128
- 984 Henry, L. G., McManus, J. F., Curry, W. B., Roberts, N. L., Piotrowski, A. M., &
 985 Keigwin, L. D. (2016, July). North Atlantic ocean circulation and abrupt cli-
 986 mate change during the last glaciation. *Science*, 353(6298), 470–474. Retrieved
 987 2020-03-04, from <https://science.sciencemag.org/content/353/6298/470>
 988 (Publisher: American Association for the Advancement of Science Section:
 989 Report) doi: 10.1126/science.aaf5529
- 990 Hodell, D. A., Nicholl, J. A., Bontognali, T. R. R., Danino, S., Dorador, J.,
 991 Dowdeswell, J. A., ... Röhl, U. (2017). Anatomy of Heinrich Layer 1 and
 992 its role in the last deglaciation. *Paleoceanography*, 32(3), 284–303. Retrieved

- 993 2020-07-15, from [https://agupubs.onlinelibrary.wiley.com/doi/abs/](https://agupubs.onlinelibrary.wiley.com/doi/abs/10.1002/2016PA003028)
994 10.1002/2016PA003028 doi: 10.1002/2016PA003028
- 995 Huber, C., Leuenberger, M., Spahni, R., Flückiger, J., Schwander, J., Stocker,
996 T. F., ... Jouzel, J. (2006, March). Isotope calibrated Greenland temper-
997 ature record over Marine Isotope Stage 3 and its relation to CH₄. *Earth*
998 *and Planetary Science Letters*, 243(3), 504–519. Retrieved 2020-06-29, from
999 <http://www.sciencedirect.com/science/article/pii/S0012821X06000392>
1000 doi: 10.1016/j.epsl.2006.01.002
- 1001 Hughes, A. L. C., Gyllencreutz, R., Lohne, Ø. S., Mangerud, J., & Svendsen, J. I.
1002 (2016). The last Eurasian ice sheets – a chronological database and time-slice
1003 reconstruction, DATED-1. *Boreas*, 45(1), 1–45. Retrieved 2020-01-27, from
1004 <https://onlinelibrary.wiley.com/doi/abs/10.1111/bor.12142> doi:
1005 10.1111/bor.12142
- 1006 I.P.C.C. (2014). Evaluation of Climate Models. In Intergovernmental Panel on
1007 Climate Change (Ed.), *Climate Change 2013 – The Physical Science Basis:*
1008 *Working Group I Contribution to the Fifth Assessment Report of the Intergov-*
1009 *ernmental Panel on Climate Change* (pp. 741–866). Cambridge: Cambridge
1010 University Press. Retrieved 2021-09-06, from [https://www.cambridge.org/](https://www.cambridge.org/core/books/climate-change-2013-the-physical-science-basis/evaluation-of-climate-models/94BC2268C864F2C6A18436DB22BD1E5A)
1011 [core/books/climate-change-2013-the-physical-science-basis/](https://www.cambridge.org/core/books/climate-change-2013-the-physical-science-basis/evaluation-of-climate-models/94BC2268C864F2C6A18436DB22BD1E5A)
1012 [evaluation-of-climate-models/94BC2268C864F2C6A18436DB22BD1E5A](https://www.cambridge.org/core/books/climate-change-2013-the-physical-science-basis/evaluation-of-climate-models/94BC2268C864F2C6A18436DB22BD1E5A)
1013 doi: 10.1017/CBO9781107415324.020
- 1014 Ivanovic, R. F., Gregoire, L. J., Burke, A., Wickert, A. D., Valdes, P. J., Ng, H. C.,
1015 ... Dentith, J. E. (2018). Acceleration of Northern Ice Sheet Melt Induces
1016 AMOC Slowdown and Northern Cooling in Simulations of the Early Last
1017 Deglaciation. *Paleoceanography and Paleoclimatology*, 33(7), 807–824. Re-
1018 trieved 2019-10-02, from [https://agupubs.onlinelibrary.wiley.com/doi/](https://agupubs.onlinelibrary.wiley.com/doi/abs/10.1029/2017PA003308)
1019 [abs/10.1029/2017PA003308](https://agupubs.onlinelibrary.wiley.com/doi/abs/10.1029/2017PA003308) doi: 10.1029/2017PA003308
- 1020 Ivanovic, R. F., Gregoire, L. J., Kageyama, M., Roche, D. M., Valdes, P. J., Burke,
1021 A., ... Tarasov, L. (2016, July). Transient climate simulations of the deglacia-
1022 tion 21–9 thousand years before present (version 1) – PMIP4 Core experiment
1023 design and boundary conditions. *Geoscientific Model Development*, 9(7), 2563–
1024 2587. Retrieved 2020-02-20, from [https://www.geosci-model-dev.net/9/](https://www.geosci-model-dev.net/9/2563/2016/)
1025 [2563/2016/](https://www.geosci-model-dev.net/9/2563/2016/) doi: <https://doi.org/10.5194/gmd-9-2563-2016>
- 1026 Ivanovic, R. F., Gregoire, L. J., Wickert, A. D., Valdes, P. J., & Burke, A. (2017).
1027 Collapse of the North American ice saddle 14,500 years ago caused widespread
1028 cooling and reduced ocean overturning circulation. *Geophysical Research*
1029 *Letters*, 44(1), 383–392. Retrieved 2020-07-09, from [https://agupubs](https://agupubs.onlinelibrary.wiley.com/doi/abs/10.1002/2016GL071849)
1030 [.onlinelibrary.wiley.com/doi/abs/10.1002/2016GL071849](https://agupubs.onlinelibrary.wiley.com/doi/abs/10.1002/2016GL071849) (eprint:
1031 <https://agupubs.onlinelibrary.wiley.com/doi/pdf/10.1002/2016GL071849>) doi:
1032 10.1002/2016GL071849
- 1033 Kageyama, M., Albani, S., Braconnot, P., Harrison, S. P., Hopcroft, P. O., Ivanovic,
1034 R. F., ... Zheng, W. (2017, November). The PMIP4 contribution to CMIP6 –
1035 Part 4: Scientific objectives and experimental design of the PMIP4-CMIP6
1036 Last Glacial Maximum experiments and PMIP4 sensitivity experiments.
1037 *Geoscientific Model Development*, 10(11), 4035–4055. Retrieved 2020-
1038 02-20, from <https://www.geosci-model-dev.net/10/4035/2017/> doi:
1039 <https://doi.org/10.5194/gmd-10-4035-2017>
- 1040 Kageyama, M., Harrison, S. P., Kapsch, M.-L., Lofverstrom, M., Lora, J. M., Miko-
1041 lajewicz, U., ... Zhu, J. (2021, May). The PMIP4 Last Glacial Maximum
1042 experiments: preliminary results and comparison with the PMIP3 simula-
1043 tions. *Climate of the Past*, 17(3), 1065–1089. Retrieved 2022-03-01, from
1044 <https://cp.copernicus.org/articles/17/1065/2021/> (Publisher: Coperni-
1045 cus GmbH) doi: 10.5194/cp-17-1065-2021
- 1046 Kageyama, M., Paul, A., Roche, D. M., & Van Meerbeeck, C. J. (2010, Oc-
1047 tober). Modelling glacial climatic millennial-scale variability related to

- 1048 changes in the Atlantic meridional overturning circulation: a review. *Qua-*
 1049 *ternary Science Reviews*, 29(21), 2931–2956. Retrieved 2020-03-05, from
 1050 <http://www.sciencedirect.com/science/article/pii/S0277379110001745>
 1051 doi: 10.1016/j.quascirev.2010.05.029
- 1052 Kapsch, M.-L., Mikolajewicz, U., Ziemer, F., & Schannwell, C. (2022). Ocean
 1053 response in transient simulations of the last deglaciation dominated by under-
 1054 lying ice-sheet reconstruction and method of meltwater distribution. *Geophys-*
 1055 *ical Research Letters*, n/a(n/a), e2021GL096767. Retrieved 2022-02-02, from
 1056 <https://onlinelibrary.wiley.com/doi/abs/10.1029/2021GL096767> doi:
 1057 10.1029/2021GL096767
- 1058 Kindler, P., Guillevic, M., Baumgartner, M., Schwander, J., Landais, A., & Leuen-
 1059 berger, M. (2014, April). Temperature reconstruction from 10 to 120 kyr
 1060 b2k from the NGRIP ice core. *Climate of the Past*, 10(2), 887–902. Re-
 1061 trieved 2021-02-10, from [https://cp.copernicus.org/articles/10/](https://cp.copernicus.org/articles/10/887/2014/cp-10-887-2014.html)
 1062 [887/2014/cp-10-887-2014.html](https://cp.copernicus.org/articles/10/887/2014/cp-10-887-2014.html) (Publisher: Copernicus GmbH) doi:
 1063 <https://doi.org/10.5194/cp-10-887-2014>
- 1064 Klockmann, M., Mikolajewicz, U., Kleppin, H., & Marotzke, J. (2020). Cou-
 1065 pling of the Subpolar Gyre and the Overturning Circulation During
 1066 Abrupt Glacial Climate Transitions. *Geophysical Research Letters*,
 1067 47(21), e2020GL090361. Retrieved 2020-12-11, from <https://agupubs>
 1068 [.onlinelibrary.wiley.com/doi/abs/10.1029/2020GL090361](https://agupubs.onlinelibrary.wiley.com/doi/abs/10.1029/2020GL090361) (eprint:
 1069 <https://agupubs.onlinelibrary.wiley.com/doi/pdf/10.1029/2020GL090361>) doi:
 1070 <https://doi.org/10.1029/2020GL090361>
- 1071 Klockmann, M., Mikolajewicz, U., & Marotzke, J. (2016, September). The effect
 1072 of greenhouse gas concentrations and ice sheets on the glacial AMOC in a
 1073 coupled climate model. *Climate of the Past*, 12(9), 1829–1846. Retrieved
 1074 2021-09-08, from <https://cp.copernicus.org/articles/12/1829/2016/>
 1075 (Publisher: Copernicus GmbH) doi: 10.5194/cp-12-1829-2016
- 1076 Klockmann, M., Mikolajewicz, U., & Marotzke, J. (2018, July). Two AMOC States
 1077 in Response to Decreasing Greenhouse Gas Concentrations in the Coupled Cli-
 1078 mate Model MPI-ESM. *Journal of Climate*, 31(19), 7969–7984. Retrieved
 1079 2019-10-02, from <https://journals.ametsoc.org/doi/full/10.1175/>
 1080 [JCLI-D-17-0859.1](https://journals.ametsoc.org/doi/full/10.1175/JCLI-D-17-0859.1) doi: 10.1175/JCLI-D-17-0859.1
- 1081 Lambeck, K. (2004, June). Sea-level change through the last glacial cycle: geo-
 1082 physical, glaciological and palaeogeographic consequences. *Comptes Ren-*
 1083 *dus Geoscience*, 336(7), 677–689. Retrieved 2021-12-20, from <https://>
 1084 www.sciencedirect.com/science/article/pii/S1631071304000896 doi:
 1085 10.1016/j.crte.2003.12.017
- 1086 Lambeck, K., Rouby, H., Purcell, A., Sun, Y., & Sambridge, M. (2014, Octo-
 1087 ber). Sea level and global ice volumes from the Last Glacial Maximum to
 1088 the Holocene. *Proceedings of the National Academy of Sciences*, 111(43),
 1089 15296–15303. Retrieved 2020-12-11, from <https://www.pnas.org/content/>
 1090 [111/43/15296](https://www.pnas.org/content/111/43/15296) (Publisher: National Academy of Sciences Section: Physical
 1091 Sciences) doi: 10.1073/pnas.1411762111
- 1092 Li, C., & Born, A. (2019, January). Coupled atmosphere-ice-ocean dynamics in
 1093 Dansgaard-Oeschger events. *Quaternary Science Reviews*, 203, 1–20. Re-
 1094 trieved 2020-02-20, from <http://www.sciencedirect.com/science/article/>
 1095 [pii/S0277379118305705](http://www.sciencedirect.com/science/article/pii/S0277379118305705) doi: 10.1016/j.quascirev.2018.10.031
- 1096 Lisiecki, L. E., & Raymo, M. E. (2005). A Pliocene-Pleistocene stack
 1097 of 57 globally distributed benthic $\delta^{18}O$ records. *Paleoceanog-*
 1098 *raphy*, 20(1). Retrieved 2020-03-13, from <https://agupubs>
 1099 [.onlinelibrary.wiley.com/doi/abs/10.1029/2004PA001071](https://agupubs.onlinelibrary.wiley.com/doi/abs/10.1029/2004PA001071) (eprint:
 1100 <https://agupubs.onlinelibrary.wiley.com/doi/pdf/10.1029/2004PA001071>) doi:
 1101 10.1029/2004PA001071
- 1102 Liu, Z., Carlson, A. E., He, F., Brady, E. C., Otto-Bliesner, B. L., Briegleb, B. P.,

- 1103 ... Zhu, J. (2012, July). Younger Dryas cooling and the Greenland climate
 1104 response to CO₂. *Proceedings of the National Academy of Sciences*, 109(28),
 1105 11101–11104. Retrieved 2020-03-15, from [https://www.pnas.org/content/](https://www.pnas.org/content/109/28/11101)
 1106 [109/28/11101](https://www.pnas.org/content/109/28/11101) (Publisher: National Academy of Sciences Section: Physical
 1107 Sciences) doi: 10.1073/pnas.1202183109
- 1108 Liu, Z., Otto-Bliesner, B. L., He, F., Brady, E. C., Tomas, R., Clark, P. U., ...
 1109 Cheng, J. (2009, July). Transient Simulation of Last Deglaciation with a New
 1110 Mechanism for Bølling-Allerød Warming. *Science*, 325(5938), 310–314. Re-
 1111 trieved 2019-10-02, from [https://science.sciencemag.org/content/325/](https://science.sciencemag.org/content/325/5938/310)
 1112 [5938/310](https://science.sciencemag.org/content/325/5938/310) doi: 10.1126/science.1171041
- 1113 Lohmann, J., & Ditlevsen, P. D. (2019, September). Objective extraction and anal-
 1114 ysis of statistical features of Dansgaard–Oeschger events. *Climate of the Past*,
 1115 15(5), 1771–1792. Retrieved 2021-01-28, from [https://cp.copernicus.org/](https://cp.copernicus.org/articles/15/1771/2019/)
 1116 [articles/15/1771/2019/](https://cp.copernicus.org/articles/15/1771/2019/) (Publisher: Copernicus GmbH) doi: [https://doi](https://doi.org/10.5194/cp-15-1771-2019)
 1117 [.org/10.5194/cp-15-1771-2019](https://doi.org/10.5194/cp-15-1771-2019)
- 1118 Loulergue, L., Schilt, A., Spahni, R., Masson-Delmotte, V., Blunier, T., Lemieux,
 1119 B., ... Chappellaz, J. (2008, May). Orbital and millennial-scale features
 1120 of atmospheric CH₄ over the past 800,000 years. *Nature*, 453(7193), 383–
 1121 386. Retrieved 2020-03-10, from [https://www.nature.com/articles/](https://www.nature.com/articles/nature06950)
 1122 [nature06950](https://www.nature.com/articles/nature06950) (Number: 7193 Publisher: Nature Publishing Group) doi:
 1123 [10.1038/nature06950](https://doi.org/10.1038/nature06950)
- 1124 Lynch-Stieglitz, J. (2017, January). The Atlantic Meridional Overturning Circu-
 1125 lation and Abrupt Climate Change. *Annual Review of Marine Science*, 9(1),
 1126 83–104. Retrieved 2020-03-04, from [https://www.annualreviews.org/doi/10](https://www.annualreviews.org/doi/10.1146/annurev-marine-010816-060415)
 1127 [.1146/annurev-marine-010816-060415](https://www.annualreviews.org/doi/10.1146/annurev-marine-010816-060415) (Publisher: Annual Reviews) doi: 10
 1128 [.1146/annurev-marine-010816-060415](https://doi.org/10.1146/annurev-marine-010816-060415)
- 1129 Löfverström, M., Caballero, R., Nilsson, J., & Kleman, J. (2014, July). Evolution
 1130 of the large-scale atmospheric circulation in response to changing ice sheets
 1131 over the last glacial cycle. *Climate of the Past*, 10(4), 1453–1471. Retrieved
 1132 2022-02-02, from <https://cp.copernicus.org/articles/10/1453/2014/>
 1133 (Publisher: Copernicus GmbH) doi: 10.5194/cp-10-1453-2014
- 1134 Manabe, S., & Stouffer, R. J. (1988, September). Two Stable Equilibria of a Cou-
 1135 pled Ocean-Atmosphere Model. *Journal of Climate*, 1(9), 841–866. Re-
 1136 trieved 2020-03-04, from [https://journals.ametsoc.org/doi/abs/10.1175/](https://journals.ametsoc.org/doi/abs/10.1175/1520-0442(1988)001%3C0841%3ATSEOAC%3E2.0.CO%3B2)
 1137 [1520-0442\(1988\)001%3C0841%3ATSEOAC%3E2.0.CO%3B2](https://journals.ametsoc.org/doi/abs/10.1175/1520-0442(1988)001%3C0841%3ATSEOAC%3E2.0.CO%3B2) (Publisher:
 1138 American Meteorological Society) doi: 10.1175/1520-0442(1988)001<0841:
 1139 TSEOAC>2.0.CO;2
- 1140 Manabe, S., & Stouffer, R. J. (1997). Coupled ocean-atmosphere model response
 1141 to freshwater input: Comparison to Younger Dryas Event. *Paleoceanography*,
 1142 12(2), 321–336. Retrieved 2020-03-08, from [https://agupubs.onlinelibrary](https://agupubs.onlinelibrary.wiley.com/doi/abs/10.1029/96PA03932)
 1143 [.wiley.com/doi/abs/10.1029/96PA03932](https://agupubs.onlinelibrary.wiley.com/doi/abs/10.1029/96PA03932) doi: 10.1029/96PA03932
- 1144 Margari, V., Gibbard, P. L., Bryant, C. L., & Tzedakis, P. C. (2009, June). Char-
 1145 acter of vegetational and environmental changes in southern Europe during
 1146 the last glacial period; evidence from Lesvos Island, Greece. *Quaternary*
 1147 *Science Reviews*, 28(13), 1317–1339. Retrieved 2021-10-26, from [https://](https://www.sciencedirect.com/science/article/pii/S0277379109000353)
 1148 www.sciencedirect.com/science/article/pii/S0277379109000353 doi:
 1149 [10.1016/j.quascirev.2009.01.008](https://doi.org/10.1016/j.quascirev.2009.01.008)
- 1150 Marzocchi, A., & Jansen, M. F. (2017, June). Connecting Antarctic sea ice to
 1151 deep-ocean circulation in modern and glacial climate simulations. *Geo-*
 1152 *physical Research Letters*, 44(12), 6286–6295. Retrieved 2021-12-17, from
 1153 <https://agupubs.onlinelibrary.wiley.com/doi/10.1002/2017GL073936>
 1154 (Publisher: John Wiley & Sons, Ltd) doi: 10.1002/2017GL073936
- 1155 Matero, I. S. O., Gregoire, L. J., Ivanovic, R. F., Tindall, J. C., & Haywood, A. M.
 1156 (2017, September). The 8.2 ka cooling event caused by Laurentide ice sad-
 1157 dle collapse. *Earth and Planetary Science Letters*, 473, 205–214. Retrieved

- 1158 2021-09-06, from <https://www.sciencedirect.com/science/article/pii/S0012821X17303205> doi: 10.1016/j.epsl.2017.06.011
- 1159
- 1160 Menviel, L., Timmermann, A., Timm, O. E., & Mouchet, A. (2011, May). De-
1161 constructing the Last Glacial termination: the role of millennial and orbital-
1162 scale forcings. *Quaternary Science Reviews*, *30*(9), 1155–1172. Retrieved
1163 2020-03-16, from <http://www.sciencedirect.com/science/article/pii/S0277379111000539> doi: 10.1016/j.quascirev.2011.02.005
- 1164
- 1165 Muglia, J., & Schmittner, A. (2015). Glacial Atlantic overturning increased by wind
1166 stress in climate models. *Geophysical Research Letters*, *42*(22), 9862–9868.
1167 Retrieved 2019-09-16, from <https://agupubs.onlinelibrary.wiley.com/doi/abs/10.1002/2015GL064583> doi: 10.1002/2015GL064583
- 1168
- 1169 Muglia, J., & Schmittner, A. (2021, April). Carbon isotope constraints on
1170 glacial Atlantic meridional overturning: Strength vs depth. *Quaternary*
1171 *Science Reviews*, *257*, 106844. Retrieved 2021-10-26, from <https://www.sciencedirect.com/science/article/pii/S0277379121000512> doi:
1172 10.1016/j.quascirev.2021.106844
- 1173
- 1174 Murton, J. B., Bateman, M. D., Dallimore, S. R., Teller, J. T., & Yang, Z. (2010,
1175 April). Identification of Younger Dryas outburst flood path from Lake Agassiz
1176 to the Arctic Ocean. *Nature*, *464*(7289), 740–743. Retrieved 2020-03-15, from
1177 <https://www.nature.com/articles/nature08954> (Number: 7289 Publisher:
1178 Nature Publishing Group) doi: 10.1038/nature08954
- 1179 Ng, H. C., Robinson, L. F., McManus, J. F., Mohamed, K. J., Jacobel, A. W.,
1180 Ivanovic, R. F., ... Chen, T. (2018, July). Coherent deglacial changes in west-
1181 ern Atlantic Ocean circulation. *Nature Communications*, *9*(1), 1–10. Retrieved
1182 2019-10-02, from <https://www.nature.com/articles/s41467-018-05312-3>
1183 doi: 10.1038/s41467-018-05312-3
- 1184 N.G.R.I.P, M. (2004, September). High-resolution record of Northern Hemisphere
1185 climate extending into the last interglacial period. *Nature*, *431*(7005), 147–
1186 151. Retrieved 2020-03-13, from <https://www.nature.com/articles/nature02805>
1187 (Number: 7005 Publisher: Nature Publishing Group) doi:
1188 10.1038/nature02805
- 1189 Obase, T., & Abe-Ouchi, A. (2019). Abrupt Bølling-Allerød Warming Sim-
1190 ulated under Gradual Forcing of the Last Deglaciation. *Geophysical*
1191 *Research Letters*, *46*(20), 11397–11405. Retrieved 2021-12-17, from
1192 <https://onlinelibrary.wiley.com/doi/abs/10.1029/2019GL084675> doi:
1193 10.1029/2019GL084675
- 1194 Oka, A., Hasumi, H., & Abe-Ouchi, A. (2012). The thermal thresh-
1195 old of the Atlantic meridional overturning circulation and its con-
1196 trol by wind stress forcing during glacial climate. *Geophysical Re-*
1197 *search Letters*, *39*(9). Retrieved 2021-09-08, from [https://agupubs](https://agupubs.onlinelibrary.wiley.com/doi/abs/10.1029/2012GL051421)
1198 [.onlinelibrary.wiley.com/doi/abs/10.1029/2012GL051421](https://agupubs.onlinelibrary.wiley.com/doi/abs/10.1029/2012GL051421) (eprint:
1199 <https://agupubs.onlinelibrary.wiley.com/doi/pdf/10.1029/2012GL051421>) doi:
1200 10.1029/2012GL051421
- 1201 Osman, M. B., Tierney, J. E., Zhu, J., Tardif, R., Hakim, G. J., King, J., & Poulsen,
1202 C. J. (2021, November). Globally resolved surface temperatures since the
1203 Last Glacial Maximum. *Nature*, *599*(7884), 239–244. Retrieved 2021-12-
1204 19, from <https://www.nature.com/articles/s41586-021-03984-4> doi:
1205 10.1038/s41586-021-03984-4
- 1206 Paillard, D., & Labeyriet, L. (1994, November). Role of the thermohaline circulation
1207 in the abrupt warming after Heinrich events. *Nature*, *372*(6502), 162–164.
1208 Retrieved 2020-02-28, from <https://www.nature.com/articles/372162a0>
1209 (Number: 6502 Publisher: Nature Publishing Group) doi: 10.1038/372162a0
- 1210 Parrenin, F., Barnola, J.-M., Beer, J., Blunier, T., Castellano, E., Chappellaz, J.,
1211 ... Wolff, E. (2007, August). The EDC3 chronology for the EPICA Dome
1212 C ice core. *Climate of the Past*, *3*(3), 485–497. Retrieved 2020-07-15, from

- 1213 <https://cp.copernicus.org/articles/3/485/2007/> (Publisher: Coperni-
1214 cus GmbH) doi: <https://doi.org/10.5194/cp-3-485-2007>
- 1215 Paul, A., Mulitza, S., Stein, R., & Werner, M. (2021, April). A global climatology
1216 of the ocean surface during the Last Glacial Maximum mapped on a regular
1217 grid (GLOMAP). *Climate of the Past*, *17*(2), 805–824. Retrieved 2021-12-19,
1218 from <https://cp.copernicus.org/articles/17/805/2021/> (Publisher:
1219 Copernicus GmbH) doi: 10.5194/cp-17-805-2021
- 1220 Peltier, W. R., Argus, D. F., & Drummond, R. (2015). Space geodesy
1221 constrains ice age terminal deglaciation: The global ICE-6G.c
1222 (VM5a) model. *Journal of Geophysical Research: Solid Earth*,
1223 *120*(1), 450–487. Retrieved 2020-03-08, from [https://agupubs
1224 .onlinelibrary.wiley.com/doi/abs/10.1002/2014JB011176](https://agupubs.onlinelibrary.wiley.com/doi/abs/10.1002/2014JB011176) (eprint:
1225 <https://agupubs.onlinelibrary.wiley.com/doi/pdf/10.1002/2014JB011176>) doi:
1226 10.1002/2014JB011176
- 1227 Peltier, W. R., & Vettoretti, G. (2014). Dansgaard-Oeschger oscillations predicted
1228 in a comprehensive model of glacial climate: A “kicked” salt oscillator in the
1229 Atlantic. *Geophysical Research Letters*, *41*(20), 7306–7313. Retrieved 2019-
1230 08-05, from [https://agupubs.onlinelibrary.wiley.com/doi/abs/10.1002/
1231 2014GL061413](https://agupubs.onlinelibrary.wiley.com/doi/abs/10.1002/2014GL061413) doi: 10.1002/2014GL061413
- 1232 Peterson, L. C., & Haug, G. H. (2006, May). Variability in the mean latitude of
1233 the Atlantic Intertropical Convergence Zone as recorded by riverine input of
1234 sediments to the Cariaco Basin (Venezuela). *Palaeoecology, Palaeoecolima-
1235 tology, Palaeoecology*, *234*(1), 97–113. Retrieved 2022-03-01, from [https://
1236 www.sciencedirect.com/science/article/pii/S0031018205006115](https://www.sciencedirect.com/science/article/pii/S0031018205006115) doi:
1237 10.1016/j.palaeo.2005.10.021
- 1238 Pope, V. D., Gallani, M. L., Rowntree, P. R., & Stratton, R. A. (2000, Febru-
1239 ary). The impact of new physical parametrizations in the Hadley Cen-
1240 tre climate model: HadAM3. *Climate Dynamics*, *16*(2), 123–146. Re-
1241 trieved 2020-07-09, from <https://doi.org/10.1007/s003820050009> doi:
1242 10.1007/s003820050009
- 1243 Rahmstorf, S. (2002, September). Ocean circulation and climate during the past
1244 120,000 years. *Nature*, *419*(6903), 207–214. Retrieved 2020-03-04, from
1245 <https://www.nature.com/articles/nature01090> (Number: 6903 Publisher:
1246 Nature Publishing Group) doi: 10.1038/nature01090
- 1247 Rasmussen, T. L., Thomsen, E., & Moros, M. (2016, February). North Atlantic
1248 warming during Dansgaard-Oeschger events synchronous with Antarctic warm-
1249 ing and out-of-phase with Greenland climate. *Scientific Reports*, *6*(1), 20535.
1250 Retrieved 2020-07-13, from <https://www.nature.com/articles/srep20535>
1251 (Number: 1 Publisher: Nature Publishing Group) doi: 10.1038/srep20535
- 1252 Reichler, T., & Kim, J. (2008, March). How Well Do Coupled Models Simulate
1253 Today’s Climate? *Bulletin of the American Meteorological Society*, *89*(3),
1254 303–312. Retrieved 2021-09-06, from [https://journals.ametsoc.org/view/
1255 journals/bams/89/3/bams-89-3-303.xml](https://journals.ametsoc.org/view/journals/bams/89/3/bams-89-3-303.xml) (Publisher: American Meteorolo-
1256 gical Society Section: Bulletin of the American Meteorological Society) doi:
1257 10.1175/BAMS-89-3-303
- 1258 Renold, M., Raible, C. C., Yoshimori, M., & Stocker, T. F. (2010, January).
1259 Simulated resumption of the North Atlantic meridional overturning cir-
1260 culation – Slow basin-wide advection and abrupt local convection. *Qua-
1261 ternary Science Reviews*, *29*(1), 101–112. Retrieved 2019-05-29, from
1262 <http://www.sciencedirect.com/science/article/pii/S0277379109003680>
1263 doi: 10.1016/j.quascirev.2009.11.005
- 1264 Roberts, W. H. G., & Valdes, P. J. (2017, May). Green Mountains and White
1265 Plains: The Effect of Northern Hemisphere Ice Sheets on the Global En-
1266 ergy Budget. *Journal of Climate*, *30*(10), 3887–3905. Retrieved 2020-06-29,
1267 from <https://journals.ametsoc.org/jcli/article/30/10/3887/106888/>

- 1268 **Green-Mountains-and-White-Plains-The-Effect-of** (Publisher: American
 1269 Meteorological Society) doi: 10.1175/JCLI-D-15-0846.1
- 1270 Roberts, W. H. G., Valdes, P. J., & Payne, A. J. (2014, November). Topogra-
 1271 phy’s crucial role in Heinrich Events. *Proceedings of the National Academy*
 1272 *of Sciences*, 111(47), 16688–16693. Retrieved 2020-07-13, from [https://](https://www.pnas.org/content/111/47/16688)
 1273 www.pnas.org/content/111/47/16688 (Publisher: National Academy of
 1274 Sciences Section: Physical Sciences) doi: 10.1073/pnas.1414882111
- 1275 Roche, D. M., Renssen, H., Paillard, D., & Levvasseur, G. (2011, June). Decipher-
 1276 ing the spatio-temporal complexity of climate change of the last deglaciation: a
 1277 model analysis. *Climate of the Past*, 7(2), 591–602. Retrieved 2020-03-16, from
 1278 <https://www.clim-past.net/7/591/2011/> (Publisher: Copernicus GmbH)
 1279 doi: <https://doi.org/10.5194/cp-7-591-2011>
- 1280 Roche, D. M., Wiersma, A. P., & Renssen, H. (2010, June). A systematic study of
 1281 the impact of freshwater pulses with respect to different geographical locations.
 1282 *Climate Dynamics*, 34(7), 997–1013. Retrieved 2019-05-29, from [https://](https://doi.org/10.1007/s00382-009-0578-8)
 1283 doi.org/10.1007/s00382-009-0578-8 doi: 10.1007/s00382-009-0578-8
- 1284 Schilt, A., Baumgartner, M., Schwander, J., Buiron, D., Capron, E., Chappellaz, J.,
 1285 ... Stocker, T. F. (2010, November). Atmospheric nitrous oxide during the
 1286 last 140,000years. *Earth and Planetary Science Letters*, 300(1), 33–43. Re-
 1287 trieved 2020-03-10, from [http://www.sciencedirect.com/science/article/](http://www.sciencedirect.com/science/article/pii/S0012821X10006023)
 1288 [pii/S0012821X10006023](http://www.sciencedirect.com/science/article/pii/S0012821X10006023) doi: 10.1016/j.epsl.2010.09.027
- 1289 Schmittner, A., Yoshimori, M., & Weaver, A. J. (2002, February). Instabil-
 1290 ity of Glacial Climate in a Model of the Ocean- Atmosphere-Cryosphere
 1291 System. *Science*, 295(5559), 1489–1493. Retrieved 2020-03-08, from
 1292 <https://science.sciencemag.org/content/295/5559/1489> (Publisher:
 1293 American Association for the Advancement of Science Section: Research Arti-
 1294 cle) doi: 10.1126/science.1066174
- 1295 Severinghaus, J. P., & Brook, E. J. (1999, October). Abrupt Climate Change
 1296 at the End of the Last Glacial Period Inferred from Trapped Air in Polar
 1297 Ice. *Science*, 286(5441), 930–934. Retrieved 2020-03-10, from [https://](https://science.sciencemag.org/content/286/5441/930)
 1298 science.sciencemag.org/content/286/5441/930 (Publisher: Amer-
 1299 ican Association for the Advancement of Science Section: Report) doi:
 1300 10.1126/science.286.5441.930
- 1301 Shackleton, N. J., Hall, M. A., & Vincent, E. (2000). Phase relationships
 1302 between millennial-scale events 64,000–24,000 years ago. *Paleoceanog-*
 1303 *raphy*, 15(6), 565–569. Retrieved 2020-03-04, from [https://agupubs](https://agupubs.onlinelibrary.wiley.com/doi/abs/10.1029/2000PA000513)
 1304 [.onlinelibrary.wiley.com/doi/abs/10.1029/2000PA000513](https://agupubs.onlinelibrary.wiley.com/doi/abs/10.1029/2000PA000513) (eprint:
 1305 <https://agupubs.onlinelibrary.wiley.com/doi/pdf/10.1029/2000PA000513>) doi:
 1306 10.1029/2000PA000513
- 1307 Sherriff-Tadano, S., & Abe-Ouchi, A. (2020, April). Roles of Sea Ice–Surface
 1308 Wind Feedback in Maintaining the Glacial Atlantic Meridional Overturning
 1309 Circulation and Climate. *Journal of Climate*, 33(8), 3001–3018. Retrieved
 1310 2022-03-01, from [https://journals.ametsoc.org/view/journals/clim/](https://journals.ametsoc.org/view/journals/clim/33/8/jcli-d-19-0431.1.xml)
 1311 [33/8/jcli-d-19-0431.1.xml](https://journals.ametsoc.org/view/journals/clim/33/8/jcli-d-19-0431.1.xml) (Publisher: American Meteorological Society
 1312 Section: Journal of Climate) doi: 10.1175/JCLI-D-19-0431.1
- 1313 Sherriff-Tadano, S., Abe-Ouchi, A., & Oka, A. (2021, January). Impact of
 1314 mid-glacial ice sheets on deep ocean circulation and global climate. *Cli-*
 1315 *mate of the Past*, 17(1), 95–110. Retrieved 2022-03-01, from [https://](https://cp.copernicus.org/articles/17/95/2021/)
 1316 cp.copernicus.org/articles/17/95/2021/ (Publisher: Copernicus GmbH)
 1317 doi: 10.5194/cp-17-95-2021
- 1318 Sherriff-Tadano, S., Abe-Ouchi, A., Yoshimori, M., Oka, A., & Chan, W.-L. (2018,
 1319 April). Influence of glacial ice sheets on the Atlantic meridional overturning
 1320 circulation through surface wind change. *Climate Dynamics*, 50(7), 2881–2903.
 1321 Retrieved 2019-08-19, from <https://doi.org/10.1007/s00382-017-3780-0>
 1322 doi: 10.1007/s00382-017-3780-0

- 1323 Singarayer, J. S., Valdes, P. J., & Roberts, W. H. G. (2017, August). Ocean domi-
 1324 nated expansion and contraction of the late Quaternary tropical rainbelt. *Sci-*
 1325 *entific Reports*, 7(1), 9382. Retrieved 2022-01-21, from [https://www.nature](https://www.nature.com/articles/s41598-017-09816-8)
 1326 [.com/articles/s41598-017-09816-8](https://www.nature.com/articles/s41598-017-09816-8) doi: 10.1038/s41598-017-09816-8
- 1327 Smeed, D. A., McCarthy, G. D., Cunningham, S. A., Frajka-Williams, E., Rayner,
 1328 D., Johns, W. E., . . . Bryden, H. L. (2014, February). Observed decline of the
 1329 Atlantic meridional overturning circulation 2004–2012. *Ocean Science*,
 1330 10(1), 29–38. Retrieved 2020-02-27, from [https://www.ocean-sci.net/10/](https://www.ocean-sci.net/10/29/2014/)
 1331 [29/2014/](https://www.ocean-sci.net/10/29/2014/) doi: <https://doi.org/10.5194/os-10-29-2014>
- 1332 Smith, R. S., & Gregory, J. M. (2009). A study of the sensitivity of ocean over-
 1333 turning circulation and climate to freshwater input in different regions of the
 1334 North Atlantic. *Geophysical Research Letters*, 36(15). Retrieved 2022-02-02,
 1335 from <https://onlinelibrary.wiley.com/doi/abs/10.1029/2009GL038607>
 1336 (_eprint: <https://onlinelibrary.wiley.com/doi/pdf/10.1029/2009GL038607>) doi:
 1337 10.1029/2009GL038607
- 1338 Snoll, B., Ivanovic, R. F., Valdes, P. J., Maycock, A. C., & Gregoire, L. J. (2022,
 1339 February). Effect of orographic gravity wave drag on Northern Hemisphere
 1340 climate in transient simulations of the last deglaciation. *Climate Dynamics*.
 1341 Retrieved 2022-03-01, from <https://doi.org/10.1007/s00382-022-06196-2>
 1342 doi: 10.1007/s00382-022-06196-2
- 1343 Stanford, J. D., Rohling, E. J., Bacon, S., Roberts, A. P., Grousset, F. E., &
 1344 Bolshaw, M. (2011, May). A new concept for the paleoceanographic
 1345 evolution of Heinrich event 1 in the North Atlantic. *Quaternary Sci-*
 1346 *ence Reviews*, 30(9), 1047–1066. Retrieved 2020-02-28, from [http://](http://www.sciencedirect.com/science/article/pii/S0277379111000400)
 1347 www.sciencedirect.com/science/article/pii/S0277379111000400 doi:
 1348 10.1016/j.quascirev.2011.02.003
- 1349 Stern, J. V., & Lisiecki, L. E. (2013, July). North Atlantic circulation and reservoir
 1350 age changes over the past 41,000 years. *Geophysical Research Letters*, 40(14),
 1351 3693–3697. Retrieved 2020-03-13, from [https://agupubs.onlinelibrary](https://agupubs.onlinelibrary.wiley.com/doi/full/10.1002/grl.50679)
 1352 [.wiley.com/doi/full/10.1002/grl.50679](https://agupubs.onlinelibrary.wiley.com/doi/full/10.1002/grl.50679) doi: 10.1002/grl.50679
- 1353 Stocker, T. F. (1998, October). The Seesaw Effect. *Science*, 282(5386), 61–62.
 1354 Retrieved 2021-11-11, from [https://www.science.org/doi/full/10.1126/](https://www.science.org/doi/full/10.1126/science.282.5386.61)
 1355 [science.282.5386.61](https://www.science.org/doi/full/10.1126/science.282.5386.61) (Publisher: American Association for the Advance-
 1356 ment of Science) doi: 10.1126/science.282.5386.61
- 1357 Stocker, T. F., & Johnsen, S. J. (2003). A minimum thermodynamic model for
 1358 the bipolar seesaw. *Paleoceanography*, 18(4). Retrieved 2021-11-11, from
 1359 <https://onlinelibrary.wiley.com/doi/abs/10.1029/2003PA000920>
 1360 (_eprint: <https://onlinelibrary.wiley.com/doi/pdf/10.1029/2003PA000920>)
 1361 doi: 10.1029/2003PA000920
- 1362 Stockhecke, M., Timmermann, A., Kipfer, R., Haug, G. H., Kwiecien, O., Friedrich,
 1363 T., . . . Anselmetti, F. S. (2016, February). Millennial to orbital-scale
 1364 variations of drought intensity in the Eastern Mediterranean. *Quater-*
 1365 *nary Science Reviews*, 133, 77–95. Retrieved 2021-10-26, from [https://](https://www.sciencedirect.com/science/article/pii/S0277379115301979)
 1366 www.sciencedirect.com/science/article/pii/S0277379115301979 doi:
 1367 10.1016/j.quascirev.2015.12.016
- 1368 Stommel, H. (1961). Thermohaline Convection with Two Stable Regimes of Flow.
 1369 *Tellus*, 13(2), 224–230. Retrieved 2020-03-04, from [https://onlinelibrary](https://onlinelibrary.wiley.com/doi/abs/10.1111/j.2153-3490.1961.tb00079.x)
 1370 [.wiley.com/doi/abs/10.1111/j.2153-3490.1961.tb00079.x](https://onlinelibrary.wiley.com/doi/abs/10.1111/j.2153-3490.1961.tb00079.x) (_eprint:
 1371 <https://onlinelibrary.wiley.com/doi/pdf/10.1111/j.2153-3490.1961.tb00079.x>)
 1372 doi: 10.1111/j.2153-3490.1961.tb00079.x
- 1373 Tarasov, L., Dyke, A. S., Neal, R. M., & Peltier, W. R. (2012, January). A data-
 1374 calibrated distribution of deglacial chronologies for the North American ice
 1375 complex from glaciological modeling. *Earth and Planetary Science Letters*,
 1376 315–316, 30–40. Retrieved 2020-03-08, from [http://www.sciencedirect.com/](http://www.sciencedirect.com/science/article/pii/S0012821X11005243)
 1377 [science/article/pii/S0012821X11005243](http://www.sciencedirect.com/science/article/pii/S0012821X11005243) doi: 10.1016/j.epsl.2011.09.010

- 1378 Tarasov, L., & Peltier, R. W. (2002, July). Greenland glacial history and lo-
 1379 cal geodynamic consequences. *Geophysical Journal International*, 150(1),
 1380 198–229. Retrieved 2020-03-10, from [https://academic.oup.com/](https://academic.oup.com/gji/article/150/1/198/591943)
 1381 [gji/article/150/1/198/591943](https://academic.oup.com/gji/article/150/1/198/591943) (Publisher: Oxford Academic) doi:
 1382 10.1046/j.1365-246X.2002.01702.x
- 1383 Thomas, E. R., Wolff, E. W., Mulvaney, R., Johnsen, S. J., Steffensen, J. P.,
 1384 & Arrowsmith, C. (2009). Anatomy of a Dansgaard-Oeschger
 1385 warming transition: High-resolution analysis of the North Greenland
 1386 Ice Core Project ice core. *Journal of Geophysical Research: Atmo-*
 1387 *spheres*, 114(D8). Retrieved 2021-01-28, from [https://agupubs](https://agupubs.onlinelibrary.wiley.com/doi/abs/10.1029/2008JD011215)
 1388 [.onlinelibrary.wiley.com/doi/abs/10.1029/2008JD011215](https://agupubs.onlinelibrary.wiley.com/doi/abs/10.1029/2008JD011215) (eprint:
 1389 <https://agupubs.onlinelibrary.wiley.com/doi/pdf/10.1029/2008JD011215>) doi:
 1390 <https://doi.org/10.1029/2008JD011215>
- 1391 Tierney, J. E., Zhu, J., King, J., Malevich, S. B., Hakim, G. J., & Poulsen, C. J.
 1392 (2020, August). Glacial cooling and climate sensitivity revisited. *Nature*,
 1393 584(7822), 569–573. Retrieved 2021-12-19, from [https://www.nature.com/](https://www.nature.com/articles/s41586-020-2617-x)
 1394 [articles/s41586-020-2617-x](https://www.nature.com/articles/s41586-020-2617-x) doi: 10.1038/s41586-020-2617-x
- 1395 Ullman, D. J., LeGrande, A. N., Carlson, A. E., Anslow, F. S., & Licciardi, J. M.
 1396 (2014, March). Assessing the impact of Laurentide Ice Sheet topography on
 1397 glacial climate. *Climate of the Past*, 10(2), 487–507. Retrieved 2021-09-08,
 1398 from <https://cp.copernicus.org/articles/10/487/2014/> (Publisher:
 1399 Copernicus GmbH) doi: 10.5194/cp-10-487-2014
- 1400 Valdes, P. J., Armstrong, E., Badger, M. P. S., Bradshaw, C. D., Bragg, F.,
 1401 Davies-Barnard, T., ... Williams, J. H. T. (2017, October). The BRIDGE
 1402 HadCM3 family of climate models: HadCM3@Bristol v1.0. *Geoscientific*
 1403 *Model Development Discussions*. Retrieved 2020-07-09, from [https://](https://research-information.bris.ac.uk/en/publications/the-bridge-hadcm3-family-of-climate-models-hadcm3bristol-v10-2)
 1404 [research-information.bris.ac.uk/en/publications/the-bridge-hadcm3](https://research-information.bris.ac.uk/en/publications/the-bridge-hadcm3-family-of-climate-models-hadcm3bristol-v10-2)
 1405 [-family-of-climate-models-hadcm3bristol-v10-2](https://research-information.bris.ac.uk/en/publications/the-bridge-hadcm3-family-of-climate-models-hadcm3bristol-v10-2) (Publisher: Copernicus
 1406 GmbH) doi: 10.5194/gmd-2017-16
- 1407 Vettoretti, G., & Peltier, W. R. (2018, May). Fast Physics and Slow Physics
 1408 in the Nonlinear Dansgaard–Oeschger Relaxation Oscillation. *Jour-*
 1409 *nal of Climate*, 31(9), 3423–3449. Retrieved 2022-01-12, from [https://](https://journals.ametsoc.org/view/journals/clim/31/9/jcli-d-17-0559.1.xml)
 1410 journals.ametsoc.org/view/journals/clim/31/9/jcli-d-17-0559.1.xml
 1411 (Important) doi: 10.1175/JCLI-D-17-0559.1
- 1412 Vidal, L., Labeyrie, L., Cortijo, E., Arnold, M., Duplessy, J. C., Michel, E., ... van
 1413 Weering, T. C. E. (1997, January). Evidence for changes in the North Atlantic
 1414 Deep Water linked to meltwater surges during the Heinrich events. *Earth*
 1415 *and Planetary Science Letters*, 146(1), 13–27. Retrieved 2020-02-28, from
 1416 <http://www.sciencedirect.com/science/article/pii/S0012821X96001926>
 1417 doi: 10.1016/S0012-821X(96)00192-6
- 1418 Voelker, A. H. L. (2002, May). Global distribution of centennial-scale
 1419 records for Marine Isotope Stage (MIS) 3: a database. *Quaternary Sci-*
 1420 *ence Reviews*, 21(10), 1185–1212. Retrieved 2020-03-04, from [http://](http://www.sciencedirect.com/science/article/pii/S0277379101001391)
 1421 www.sciencedirect.com/science/article/pii/S0277379101001391 doi:
 1422 10.1016/S0277-3791(01)00139-1
- 1423 Wang, X., Auler, A. S., Edwards, R. L., Cheng, H., Ito, E., Wang, Y., ... Solheid,
 1424 M. (2007). Millennial-scale precipitation changes in southern Brazil over the
 1425 past 90,000 years. *Geophysical Research Letters*, 34(23). Retrieved 2021-10-26,
 1426 from <https://onlinelibrary.wiley.com/doi/abs/10.1029/2007GL031149>
 1427 doi: 10.1029/2007GL031149
- 1428 Wang, Y. J., Cheng, H., Edwards, R. L., An, Z. S., Wu, J. Y., Shen, C.-C., & Do-
 1429 rale, J. A. (2001, December). A High-Resolution Absolute-Dated Late Pleis-
 1430 tocene Monsoon Record from Hulu Cave, China. *Science*, 294(5550), 2345–
 1431 2348. Retrieved 2021-10-21, from [https://www.science.org/doi/10.1126/](https://www.science.org/doi/10.1126/science.1064618)
 1432 [science.1064618](https://www.science.org/doi/10.1126/science.1064618) (Publisher: American Association for the Advancement of

- 1433 Science) doi: 10.1126/science.1064618
1434 Weber, M. E., Clark, P. U., Kuhn, G., Timmermann, A., Sprenk, D., Gladstone, R.,
1435 ... Ohlwein, C. (2014, June). Millennial-scale variability in Antarctic ice-sheet
1436 discharge during the last deglaciation. *Nature*, *510*(7503), 134–138. Retrieved
1437 2021-09-06, from <https://www.nature.com/articles/nature13397> doi:
1438 10.1038/nature13397
1439 Wolff, E. W., Chappellaz, J., Blunier, T., Rasmussen, S. O., & Svensson, A. (2010,
1440 October). Millennial-scale variability during the last glacial: The ice core
1441 record. *Quaternary Science Reviews*, *29*(21), 2828–2838. Retrieved 2020-
1442 03-04, from [http://www.sciencedirect.com/science/article/pii/
1443 S0277379109003588](http://www.sciencedirect.com/science/article/pii/S0277379109003588) doi: 10.1016/j.quascirev.2009.10.013
1444 Zhang, X., Knorr, G., Lohmann, G., & Barker, S. (2017, July). Abrupt North
1445 Atlantic circulation changes in response to gradual CO₂ forcing in a glacial
1446 climate state. *Nature Geoscience*, *10*(7), 518–523. Retrieved 2019-10-02, from
1447 <https://www.nature.com/articles/ngeo2974> doi: 10.1038/ngeo2974